Pergamon

Geochimica et Cosmochimica Acta, Vol. 68, No. 21, pp. 4429–4451, 2004

0016-7037/04 $30.00 + .00

doi:10.1016/j.gca.2004.04.027

# Geochemistry of Peruvian near-surface sediments

Philipp Böning,[1] Hans-Jürgen Brumsack,[1,*] Michael E. Böttcher,[2] Bernhard Schnetger,[1] Cornelia Kriete,[3] Jens Kallmeyer[2,‡] and Sven Lars Borchers[1]

[1]Institute of Chemistry and Biology of the Marine Environment (ICBM), Carl von Ossietzky University of Oldenburg, P.O. Box 2503, D-26111 Oldenburg, Germany
[2]Max Planck Institute for Marine Microbiology, Celsiusstrasse 1, D-28359 Bremen, Germany
[3]Federal Institute for Geosciences and Natural Resources (BGR), Stilleweg 2, D-30655 Hannover, Germany

(*Received May* 27, 2003; *accepted in revised form April* 23, 2004)

**Abstract**—Sixteen short sediment cores were recovered from the upper edge (UEO), within (WO) and below (BO) the oxygen minimum zone (OMZ) off Peru during cruise 147 of R/V *Sonne*. Solids were analyzed for major/trace elements, total organic carbon, total inorganic carbon, total sulfur, the stable sulfur isotope composition ($\delta^{34}S$) of pyrite, and sulfate reduction rates (SRR). Pore waters were analyzed for dissolved sulfate/sulfide and $\delta^{34}S$ of sulfate. In all cores highest SRR were observed in the top 5 cm where pore water sulfate concentrations varied little due to resupply of sulfate by sulfide oxidation and/or diffusion of sulfate from bottom water. $\delta^{34}S$ of dissolved sulfate showed only minor downcore increases. Strong $^{32}S$ enrichments in sedimentary pyrite (to −48‰ vs. V-CDT) are due to processes in the oxidative part of the sulfur cycle in addition to sulfate reduction. Manganese and Co are significantly depleted in Peruvian upwelling sediments most likely due to mobilization from particles settling through the OMZ, whereas release of both elements from reducing sediments only seems to occur in near-coastal sites. Cadmium, Mo and Re are exceptionally enriched in WO sediments (<600 m water depth). High Re and moderate Cd and Mo enrichments are seen in BO sediments (>600 m water depth). Re/Mo ratios indicate anoxic and suboxic conditions for WO and BO sediments, respectively. Cadmium and Mo downcore profiles suggest considerable contribution to UEO/WO sediments by a biodetrital phase, whereas Re presumably accumulates via diffusion across the sediment-water interface to precipitation depth. Uranium is distinctly enriched in WO sediments (due to sulfidic conditions) and in some BO sediments (due to phosphorites). Silver transfer to suboxic BO sediments is likely governed by diatomaceous matter input, whereas in anoxic WO sediments Ag is presumably trapped due to sulfide precipitation. Cadmium, Cu, Zn, Ni, Cr, Ag, and T1 predominantly accumulate via biogenic pre-concentration in plankton remains. Rhenium, Sb, As, V, U and Mo are enriched in accordance with seawater TE availability. Lead and Bi enrichment in UEO surface sediments is likely contributed by anthropogenic activity (mining). Accumulation rates of TOC, Cd, Mo, U, and V from Peruvian and Namibian sediments exceed those from the Oman Margin and Gulf of California due to enhanced preservation off Peru and Namibia. 

## 1. INTRODUCTION

The continental margin beneath the highly productive Peruvian upwelling system forms a major sink for decaying organic material (e.g., Krissek et al., 1980; Scheidegger and Krissek, 1983). Sediments from basins between 10° and 14°S typically consist either of diatomaceous mud or of fine-grained clay enriched in organic carbon, phosphate, biogenic opal and carbonate (Krissek et al., 1980). Upwelling induced productivity off Peru causes an intense oxygen minimum zone (OMZ < 5 $\mu$M $O_2$; Brockmann et al., 1980) in water depths ~50–650 m (Emeis et al., 1991; Lückge and Reinhardt, 2000) along the shelf and upper slope. Particle transfer through these $O_2$-deficient waters mainly occurs as aggregated organic/inorganic material in fecal pellets besides direct settling of suspended material (Krissek et al., 1980; Brodie and Kemp, 1995). Particle sorting/fixation is not only governed by undercurrent activities (Reimers and Suess, 1983; Reinhardt et al., 2002) but also by extensive bacterial mats and fluff layers (e.g., Fossing, 1990). The sediments show complex laminations caused by variations in biogenic and detrital fluxes and bottom water oxygenation. However, mm-scale lamination is scarce within near-surface sediments (Brodie and Kemp, 1994).

Upwelling off Peru is perennial, wind–driven, and presently concentrated in the zones 7°–8°S, 11°–12°S and 14°–16°S (Suess et al., 1986). The hydrography of the Peruvian upwelling system is dominated by two currents (e.g., Hill et al., 1998, and references therein): the equator-ward $O_2$-rich Peru Chile Current and the pole-ward undercurrent. The nutrient-rich, $O_2$-deficient undercurrent flows from 5°S to 15°S, and touches the sea floor between 150–400 m water depth. At present, the undercurrent reaches its highest velocity at 10°S leading to partial erosion of the elongated shelf (Reimers and Suess, 1983) whereas velocities are far lower between 11°S and 14°S allowing sediment deposition on the steeper shelf and slope (Suess et al., 1986).

* Author to whom correspondence should be addressed (brumsack@icbm.de).
† *Present address:* CEREGE UMR 6635, Europôle de l'Arbois BP80, 13545 Aix-en-Provence cdx4, France.
‡ *Present address:* Geoforschungszentrum Potsdam, Telegrafenberg, D-14473 Potsdam, Germany.

Abbreviations used: SRR = sulfate reduction rates; BSR = bacterial sulfate reduction; OM = organic matter; OMZ = oxygen minimum zone; UEO = upper edge of OMZ; WO = within OMZ; BO = below OMZ; TM = terrigenous material; TE = trace elements; SR = sedimentation rates; SWI = sediment-water interface; AR = accumulation rates.

Recent upwelling sediments from, e.g., the Gulf of California (Brumsack, 1989), the Oman Margin (Morford and Emerson, 1999) and Namibia Margin (Calvert and Price, 1983) show enrichments in many trace metals (e.g., Ag, As, Cd, Cu, Cr, Ni, Mo, Re, Sb, U, V, Zn). These enrichments are the consequence of high productivity and/or enhanced preservation in the reducing environments. Trace metal data for Peruvian upwelling sediments are rather scarce. Koide et al. (1986) presented data for Peruvian anoxic sediments and phosphorites, which show a strong enrichment in e.g., Mo, Re, and Ag. Von Breymann et al. (1990) and Emeis et al. (1990) presented a geochemical characterization of Peruvian upwelling sediments since the Miocene/Pliocene (ODP Leg 112). They tested the role of Br, Fe, and total reduced sulfur as indicators of early diagenetic processes related to OM remineralization. Arthur and Sageman (1994) reviewed the applicability of geochemical indicators of conditions promoting black shale deposition using data from Peruvian sediments. The highly sulfidic nature of Peruvian near-coastal upwelling sediments was pointed out by Emeis and Morse (1990) and Raiswell and Canfield (1996) on ODP samples, as well as by Fossing (1990) and Suits and Arthur (2000) on near-surface samples.

The aim of the present study is to provide a multi-element set of geochemical data for near-surface Peruvian upwelling sediments to (a) evaluate the spatial distribution patterns of major and trace elements with respect to their sources and mobility upon early diagenesis, (b) to illuminate the coupling of trace elements to the carbon and sulfur cycles and (c) to compare characteristic Peruvian trace metal signatures with those from other upwelling areas.

## 2. MATERIAL AND METHODS

### 2.1. Sampling Material

Sediment cores were recovered during cruise 147 of R/V *Sonne* (Kudrass, 2000). The location of the different sites and general information are given in Figure 1 and Table 1. Cores from the shallow shelf (cores 2MC, 5MC, 29MC, 120MC, and 126MC; 80–115 m water depth) are located at the *u*pper *e*dge of the *O*MZ (UEO). In these water depths the OMZ is well established (<10 $\mu$M $O_2$; CTD measurements by Lückge and Reinhardt, 2000) but the concentration of bottom water $O_2$ may reach higher levels during El Niño intervals (e.g., Levin et al., 2002). Sites from *w*ithin the *O*MZ (WO) are located on the lower shelf and upper slope (120–600 m water depth; cores 18MC, 45MC, 71MC, 104MC and 122MC). At these sites the influence of the OMZ is strong (<5 $\mu$M $O_2$; Lückge and Reinhardt, 2000). Sites from *b*elow the *O*MZ (BO) (cores 35MC, 14MC, 33MC, and 81MC; 600–1400 m water depth) are located on the lower continental slope. Here, bottom water oxygen concentrations are higher (>10 $\mu$M $O_2$; Lückge and Reinhardt, 2000).

The sediments are typically composed of partly laminated diatomaceous or diatom bearing muds. Three cores are foraminifera bearing muds (Table 1). For high-resolution analysis, sampling was done at 0.5 or 1 cm intervals. Selected samples were squeezed for pore water analyses (see 2.4.). The (solid phase) samples were stored in polyethylene bags, sealed, and immediately frozen. In the laboratory the samples were freeze-dried and homogenized in an agate mill.

### 2.2. Major Trace Elements

All samples were analyzed for the major elements Si, Al, Ti, Fe, Na, Ca, K, P, and the TE As, Cr, Cu, Mo, Mn, Ni, Pb, Sr, U, V, Y, Zn, Zr by XRF using a Philips PW 2400 X-ray spectrometer. 600 mg of sample were mixed with 3600 mg lithiumtetraborate ($Li_2B_4O_7$, Spektromelt), preoxidized at 500°C with $NH_4NO_3$ (p.a.) and fused to glass-beads. XRF measurements were done according to Schnetger et al. (2000) at the ICBM. Analytical precision was better than 2% for major elements, better than 3% for P and better than 5% for TE.

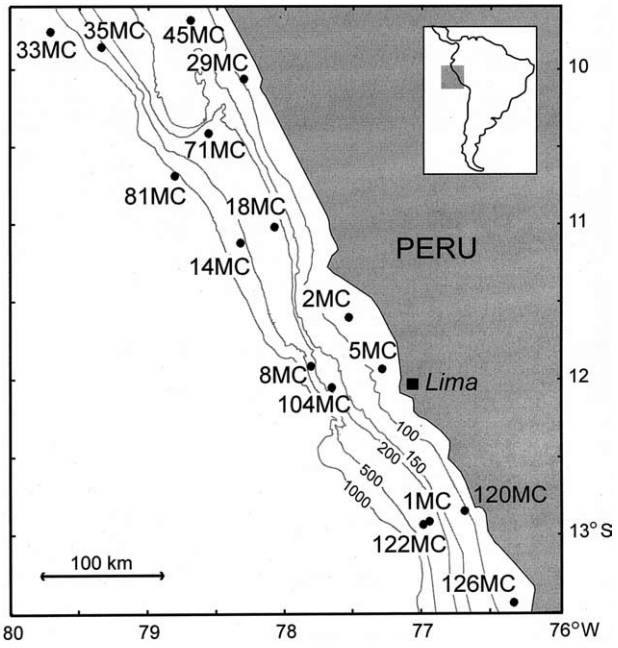


Fig. 1. Map showing sampling locations during cruise R/V *Sonne* 147 (June 2000).

ICP-MS (Finnigan MAT Element) was used to analyze for TE (Ag, Bi, Cd, Co, Cr, Cu, Mo, Ni, Pb, Re, Sb, Tl, U, Y) in acid digestions, performed according to Heinrichs and Hermann (1990) in closed PTFE vessels (PDS-6; Heinrichs et al., 1986). The samples (50 mg) were treated with 1 mL $HNO_3$ over night to oxidize organic matter. After that 3 mL HF and 3 mL $HClO_4$ were added and the vessels were heated for 12 h at 180°C. $HNO_3$ and $HClO_4$ were purified by subboiling distillation while HF was of suprapure quality. After digestion acids were evaporated on a heated metal block (180°C), residues were redissolved and fumed off three times with 3 mL half-concentrated HCl, followed by redissolution with 1 mL conc. $HNO_3$ and dilution to 50 mL. ICPMS measurements were done according to Schnetger (1997) at the ICBM. In low resolution, the isotopes $^{107}$Ag ($^{91}$Zr), $^{109}$Ag ($^{93}$Nb), $^{111}$Cd ($^{95}$Mo) and $^{114}$Cd ($^{98}$Mo) were corrected for oxide interferences (interfering isotopes in brackets). Oxide formation was calculated after analyzing a solution containing solely the interfering isotopes after blank subtraction. Typical oxide formation was low (0.3–0.8%) for Zr, Nb and Mo due to two cooled spray chambers connected to each other. Analytical precision (checked with international standards GSD-3, GSD-12, PACS-1 and several in-house standards) was better than 5% for Bi, Co, Mo, Rb, Re, Sb, Tl, better than 7% for Cd, Cu, Ni, Pb, U, V, Y, Zn and 11% for Ag. All XRF/ICP-MS data were corrected for pore water salt.

### 2.3. Carbon and Sulfur

Total sulfur (TS) and total carbon (TC) were analyzed using a Leco SC-444 IR-analyzer while total inorganic carbon (TIC) was determined coulometrically by a CM 5012 $CO_2$ coulometer coupled to a CM 5130 acidification module (Huffman, 1977; Engleman et al., 1985). Total organic carbon (TOC) was calculated as the difference between TC and TIC. The precision of bulk parameter measurements was checked in series of double runs and accuracy was determined by using in-house standards as described in Prakash Babu et al. (1999). Analytical precision was better than 3% for TC and TIC, and 5% for TS. All data were corrected for pore water contributions. According to Suits and Arthur (2000) pyrite forms the largest pool of solid-phase sulfur in surface sediments off Peru. Whereas acid-volatile sulfur (AVS) contents are always low (below 0.04 wt%),

Table 1. Summary of sampling sites and general lithology.

| Site | Position | | Water depth (m) | Core length (cm) | General lithology | Site position relative to OMZ |
|---|---|---|---|---|---|---|
| | Latitiude | Longitude | | | | |
| 126MC | 13°30.86 | 76°16.97 | 85 | 0-49 | diatom bearing mud | upper edge OMZ |
| 2MC | 11°34.97 | 77°33.08 | 86 | 0-39 | diatom bearing mud | upper edge OMZ |
| 5MC | 11°56.95 | 77°18.04 | 96 | 0-46 | diatom bearing mud | upper edge OMZ |
| 29MC | 10°03.28 | 78°17.10 | 102 | 0-49 | diatom bearing mud | upper edge OMZ |
| 120MC | 12°50.77 | 76°42.06 | 115 | 0-41 | diatom bearing mud | upper edge OMZ |
| 45MC | 9°41.47 | 78°40.99 | 153 | 0-44 | diatom bearing mud | within OMZ |
| 104MC | 12°03.68 | 76°39.84 | 185 | 0-47 | diatom bearing mud | within OMZ |
| 71MC | 10°22.42 | 78°33.51 | 239 | 0-47 | foraminifera bearing mud | within OMZ |
| 18MC | 11°01.82 | 78°04.83 | 255 | 0-46 | diatom bearing mud | within OMZ |
| 8MC | 11°54.39 | 77°49.70 | 282 | 0-34 | diatom bearing mud | within OMZ |
| 1MC | 12°55.21 | 76°58.25 | 321 | 0-40 | diatom bearing mud | within OMZ |
| 122MC | 12°55.54 | 77°00.15 | 364 | 0-39 | diatom bearing mud | within OMZ |
| 35MC | 9°51.15 | 79°20.32 | 598 | 0-19 | foraminifera bearing mud | below OMZ |
| 14MC | 11°08.00 | 78°21.33 | 654 | 0-21 | foraminifera-rich mud | below OMZ |
| 81MC | 10°40.04 | 78°51.15 | 1278 | 0-16 | silty mud | below OMZ |
| 33MC | 9°44.56 | 79°44.22 | 1357 | 0-30 | (diatom bearing) mud | below OMZ |

organic sulfur contributes ~0.1 to 0.2 wt% (Suits and Arthur, 2000). Low AVS contents were confirmed via a two-step distillation procedure.

### 2.4. Pore Water Sulfate and Sulfide Concentrations

After recovery, the cores from the multicorer were taken immediately to the cool lab (~4°C) and extruded from the liner. The disturbed outer part of the core was removed, the inner part cut into slices 0.5 cm to 2 cm thick and transferred to the 125 mL HD-PTFE containers of the pore-water press described in detail by Kriete et al. (2004). Pore water was squeezed from the core samples under a 4–8 bar argon atmosphere through 0.45 $\mu$m cellulose nitrate filters and collected directly in 25 mL argon-flushed containers for storage. Immediately after extraction, total dissolved sulfide (here termed $H_2S$) in the pore water samples was determined with an AMT picoamperemeter using an $H_2S$ microsensor. Sulfate was analyzed onboard within 24 h after sampling by ion chromatography (DIONEX IC 20). Accuracy (checked with IAPSO seawater standard) was better than 2%.

### 2.5. Stable Sulfur Isotopes ($\delta^{34}S$)

Stable sulfur isotope ratios of chromium reducible and sulfate sulfur were measured on silver sulfide and barium sulfate samples, respectively, by means of combustion-isotope-ratio-monitoring mass spectrometry (C-irmMS). $^{34}S/^{32}S$ isotope ratios were measured using an elemental analyzer (Carlo Erba EA1108 or EuroVector) coupled via a Finnigan MAT Conflo II interface to a triple collector gas mass spectrometer (Finnigan MAT 252, or ThermoFinnigan Delta+). International silver sulfide (IAEA-S-1, −2, −3) and barium sulfate (NBS 127) standards were used for calibration. Isotope ratios are given in the $\delta$-notation with respect to the $SF_6$-based V-CDT standard (Ding et al., 2001). Analytical precision was ±0.5‰.

### 2.6. Sulfate Reduction Rates (SRR)

SRR were determined using the whole-core $^{35}SO_4^{2-}$ radiotracer method of Jørgensen (1978). The subsampling technique is described by Ferdelman et al. (1997). In cases where bacterial mats covered the surface, the diameter of the tube was first cut with a scalpel to prevent destruction of the sedimentary structure. The incorporation of $^{35}SO_4^{2-}$ radiotracer into reduced sulfur species (total reduced inorganic sulfur, TRIS) consisting of acid volatile sulfur (AVS, dissolved sulfide and monosulfides) and chromium reducible sulfur (CRS, pyrite and elemental sulfur) was determined using the single step chromium reduction method of Fossing and Jørgensen (1989). Radioactivity was determined by a liquid scintillation counter (Packard 2500 TR), using Lumasafe Plus (Lumac BV, Holland) scintillation cocktail. Analytical precision was better than 5%. By comparing the activity of the radiolabeled TRIS to the total sulfate radiotracer, the sulfate reduction rate was calculated.

## 3. RESULTS AND DISCUSSION

### 3.1. Lithogenic Background for Peruvian Upwelling Sediments

The provenance of the terrigenous material (TM) delivered to the study area is (i) the arid Peruvian Andes (Clapperton 1993) and (ii) the Atacama desert from which quartz-rich eolian dust is spread NW by trade winds (Molina-Cruz, 1977). The terrigenous-detrital input is either introduced by small rivers and/or as eolian dust (Molina-Cruz, 1977; Reimers and Suess, 1983; Clapperton, 1993). However, terrigenous sediment flux calculations of Lyle (1981) and Zuta and Guillen (1970) as well as mineralogical studies of Scheidegger and Krissek (1982) indicate that Peruvian rivers dominate TM supply to the margin and significantly dilute eolian near-shore dust input.

According to Atherton and Sanderson (1985) the western slopes of the Peruvian Andes North of 14°S are comprised of granodioritic plutons, such as the Cordillera Blanca Batholith and the Coastal Batholith. Although the composition of batholiths (and corresponding volcanic extrusions) show some regional chemical variation from basic to acidic (Atherton and Sanderson, 1985) the overall chemical TM composition delivered to Peruvian sediments is andesitic. To test whether an average andesitic composition corresponds to the lithogenic background all data were plotted in the ternary diagram $Al_2O_3$-MgO · 2-$K_2O$ · 2 (Fig. 2a). Mg and K were used since they are concentrated to different degrees in igneous rocks; e.g., basaltic rocks have a higher Mg/Al and lower K/Al ratios compared to rhyolitic rocks. Moreover, Al, K, and Mg are not subject to early-diagenetic alteration processes. Mg-carbonate (dolomite) formation is not observed in the sediments since neither total Mg nor nonterrigenous Mg correlates with TIC or carbonate-Ca (not shown). Figure 2a shows that all samples plot close to andesites. The enrichment in K and Mg in core 81MC may be due to the presence of glauconite (Arthur et al., 1998).

The uniform composition of the TM in the sediments also becomes apparent from the rather indistinguishable Ti/Al and

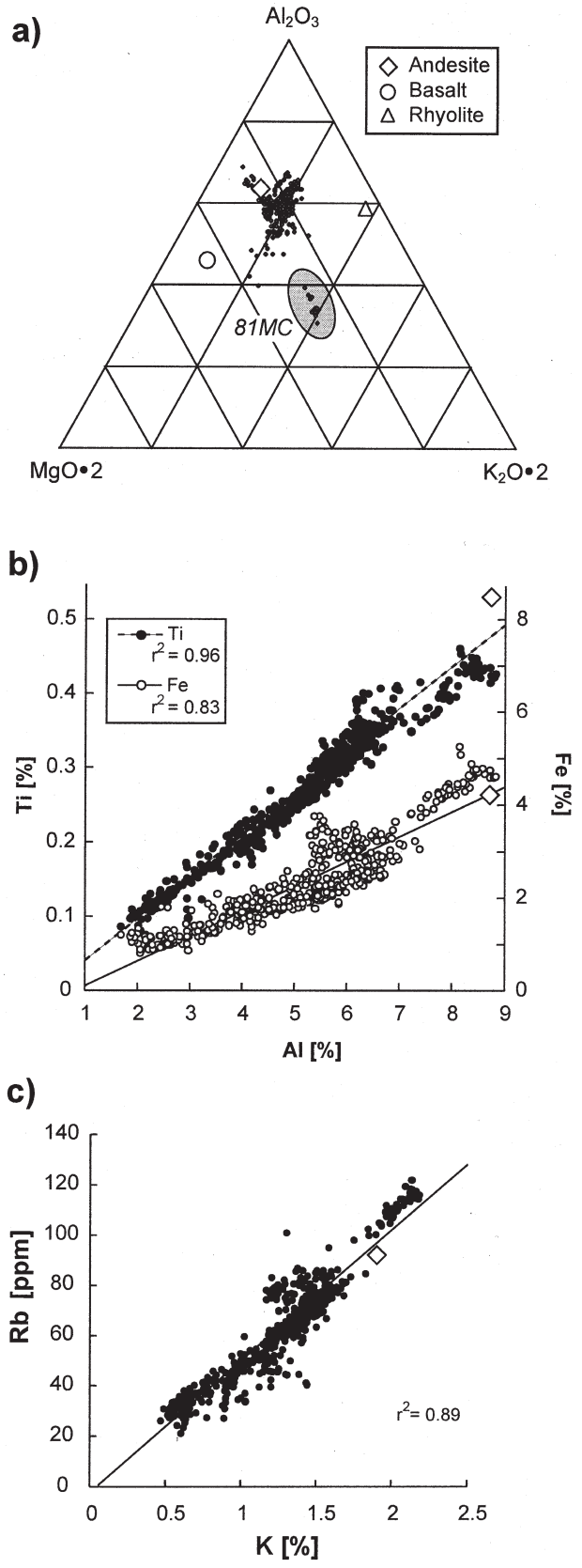


Fig. 2. (a) Terrigenous components of Peruvian upwelling sediments in the system $Al_2O_3$-MgO · 2-$K_2O$ · 2 (relative weight ratios). Data points of andesites, basalts, and ryholites (Le Maitre, 1976, also shown for comparison. 81MC = glauconite-rich sediments (presumably turbiditic; Dullo et al., 2000). (b) Correlation of Ti, Fe and Al. (c) Correlation of K and Rb. For all plots: n = 645.

K/Rb ratios (Figs. 2b,c), which are both commonly used to discern detrital matter provenance (e.g., Shimmield, 1992).

### 3.2. Geochemical Characterization of Peruvian Upwelling Sediments

The chemistry of upwelling sediments is typically dominated by five components: terrigenous material (TM), organic matter (represented by TOC), biogenic carbonate ($CaCO_3$), phosphate (or phosphorites), and biogenic silica (opal). For a chemical characterization of the sediments we use the contents of TOC, opal (opal data from Wolf, 2002) and $CaCO_3$ (Figs. 3a–c). Zr/Al ratios (Fig. 3d) are sensitive to influences of current activities (sediment reworking or winnowing) since Zr is typically enriched in the heavy mineral fraction. Phosphorus contents indicate the proportions of productivity-related and/or phosphoritic P (Fig. 3e). Phosphorites are generally associated with reworked sediments (e.g., Suess, 1981) so that higher P contents may also indicate physical sediment reworking.

Highest TOC contents are found in sediments from WO sites whereas BO and UEO sites exhibit lower TOC values (Fig. 3a), comparable to those reported in previous studies (Reimers and Suess, 1983; Lückge et al., 1996; Arthur et al., 1998). TOC flux is expected to be highest for near-coastal sites (as indicated by TOC accumulation rates in Reimers and Suess, 1983), since high SR and a shallow depth inhibit dissolution of biologic particles in the water column, and TOC may be rapidly buried and escapes aerobic decomposition (e.g., Canfield, 1994, and references therein). However, TOC values for UEO sediments are rather low (Fig. 3a) which may be due to clastic dilution and/or anaerobic decomposition of OM by bacterial sulfate reduction (BSR; see section 3.3). The peak in TOC contents (Fig. 3a) corresponds to the impingement of the most intense oxygen deficits within the OMZ (Lückge and Reinhardt, 2000) and may be the result of better OM preservation under oxygen-deficient conditions. The lower TOC contents in BO sediments may be the result of reduced OM supply due to a deeper water column and/or a preferential pole-ward OM export with the undercurrent (Reimers and Suess, 1983). Furthermore, reduced preservation may prevail due to higher $O_2$ levels in bottom waters (Lückge and Reinhardt, 2000), stronger current velocities and bioturbation leading to sediment reworking. However, Arthur et al. (1998) and Lückge et al. (1996) reported relatively high TOC contents for deeper sediments (~1000 m water depth) and ODP Site 688 (>3500 m water depth; ODP Leg 112), supporting the hypothesis that rapid resedimentation processes (turbidites) are as important for considerable OM accumulation along continental margins as primary production in surface waters.

Offshore, opal contents decrease while $CaCO_3$ contents increase (Figs. 3b,c). This distribution pattern may be explained by onshore high nutrient induced diatom production and off-

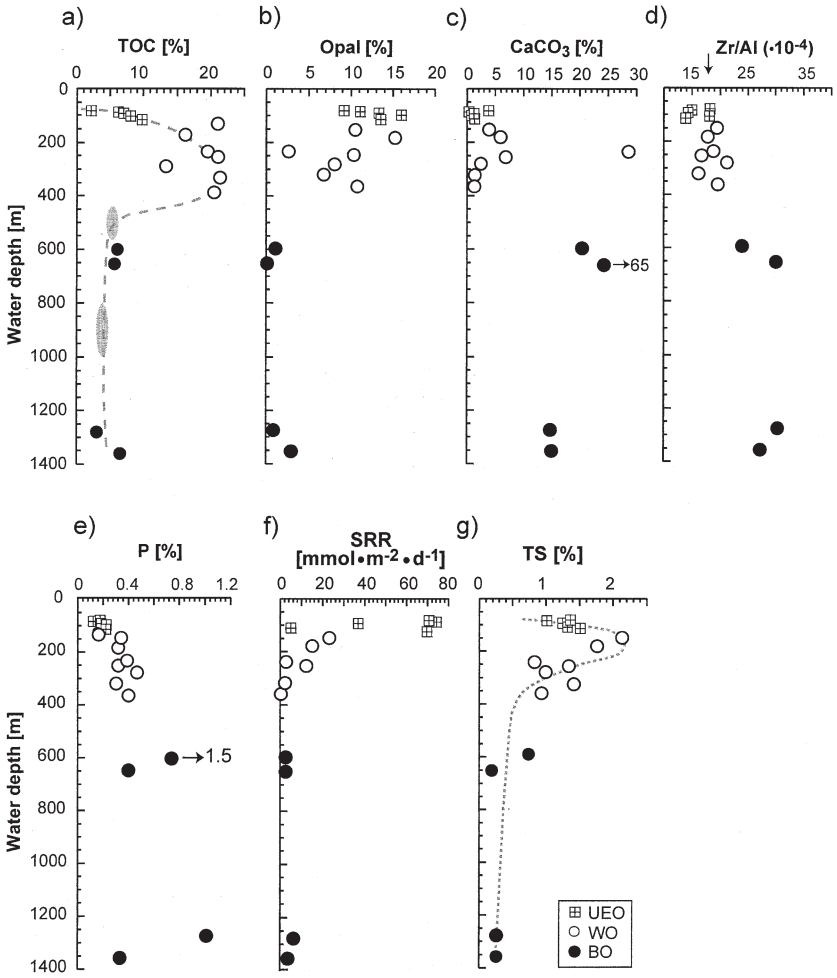


Fig. 3. Water depth profiles for (a) TOC, (b) opal (data from Wolf, 2002), (c) $CaCO_3$, (d) Zr/Al ratios, (e) phosphorus, (f) depth integrated sulfate reduction rates (SRR, 0–20 cmbsf; average of two parallel cores), (g) TS. Each data point represents the average value (solide phase) for the upper 5 cm of a single investigated core (except (b) average value from 0 to 2 cmbsf). See also Appendix for data. Dashed line = TOC smooth curve, dotted line = sulfur smooth curve. Al-normalized TOC, TS, P profiles display the same trend (not shown) as (a), (e) and (g). Shaded area in plot a) represents surface TOC data from Arthur et al. (1998). Vertical arrow in d) displays background ratio. Symbols: Windows = UEO (Upper Edge OMZ); open circles = WO (Within OMZ); filled circles = BO (Below OMZ).

shore lower nutrient induced calcareous production (Heinze and Wefer, 1992; Dullo et al., 2000; Wolf, 2002). Similarly to $CaCO_3$, Zr/Al ratios increase with water depth (Fig. 3d). Ratios equal or below average andesite ($18 \cdot 10^{-3}$) indicate the fine-grained character of UEO/WO sediments. Higher Zr/Al ratios imply that the carbonate-bearing sediments also contain a significant amount of coarse-grained material reflecting the influence of reworking/winnowing most likely by enhanced bottom currents. These findings are in agreement with those of Reimers and Suess (1983) and Wolf (2002) who also found a covariance of carbonate and coarse material influenced by bottom currents.

Phosphorus contents increase with increasing water depth (Fig. 3e). The near-shore clastic dilution may explain low P contents. Phosphorus is primarily contributed to Peruvian sediments as biodetritus (fecal pellets, plankton remains, fish debris) from productive surface waters and may accumulate as phosphorites in reworked sediments at greater water depths (e.g., Müller and Suess, 1979; Suess, 1981; Glenn and Arthur, 1988). Downcore isolated P excursions are attributed to phosphorite nodules within individual layers, especially from P-rich BO cores.

Phosphorus is preferentially remineralized relative to TOC in biodetritus settling through the water column (e.g., Müller and Suess, 1979) resulting in increased TOC/P ratios (TOC/P = 106:0.58; Knauer et al., 1979; Collier and Edmond, 1984). Higher TOC/P ratios of sedimentary OM (e.g., TOC/P = 106:0.23 for Southern Peru margin samples; Müller and Suess, 1979) indicate the continued P remineralization within the sediments. Preferential P loss is even higher when bottom waters are depleted in $O_2$ and Fe-(hydr)oxides which scavenge phosphate are dissolved within anoxic sediments (Ingall and Jahnke, 1994).

As shown in Figure 4a,b many samples from WO/UEO sites plot below the $TOC/P_{marine\ plankton}$ ratio, rather close to the ratio of water column biodetritus (TOC/p = 106:0.58; Knauer et al., 1979; Collier and Edmond, 1984) confirming the selec-

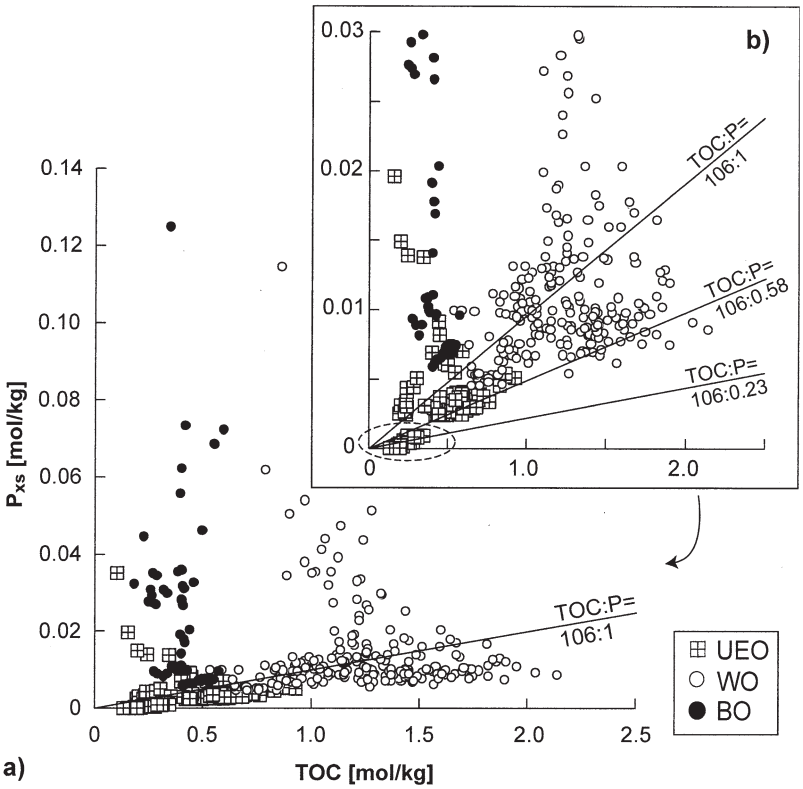


Fig. 4. (a) Scatter plots of $P_{xs}$ vs. TOC. (b) Blow-up of (a). Excess phosphorus ($P_{xs}$) was calculated as $P_{sample}$-($P/Al_{andesite} \cdot Al_{sample}$) to remove inorganic P fraction. See text for details and Figure 3 for symbols.

tive premineralization. However, only TOC/P values from the southernmost core (envelope in Fig. 4b) are close to those reported by Müller and Suess (1979). All samples from BO and some from WO/UEO show enrichments in P relative to TOC since they plot above the "marine plankton line" (Fig. 4). For UEO sites this may indicate an inherited TOC/P ratio from biodetritus due to fast accumulation. The P source for samples with low TOC/P ratios seems to be pore water phosphate and/or hydroxyapatite from fish debris as proposed by Suess (1981) for greater water depth sites. However, winnowing of less dense material (indicated by higher Zr/Al ratios; Fig. 3d) is essential for the preferential P enrichment in phosphorites (Suess, 1981; Glenn and Arthur, 1988).

### 3.3. Sedimentary Sulfur Biogeochemistry

The biogeochemistry of sulfur was investigated in sediment cores at stations 29MC, 45MC, 18MC, 14MC, and 33MC (Fig. 1, Table 1) recovered from water depths covering the whole range of bottom water $O_2$ conditions. Except for the deepest sites (14MC and 33MC) pore water concentrations of dissolved sulfate decrease slightly with depth (Fig. 5a) and show a corresponding shift to heavier values for residual sulfate $\delta^{34}S_{sulfate}$ compared to bottom water sulfate (Fig. 5d). This indicates minor net sulfate reduction. Results are comparable to those found for the upwelling area off Chile and on the NW shelf of the Black Sea (Table 2; Fig. 5d). The observed trends are in general agreement with the gross activity of sulfate reducing bacteria, measured at these stations using radio-labeled sulfate (Fig. 3f). Highest gross SRR were determined for the upper 5 cm of the cores. Depth integrated SRR show maximum values at UEO sites but decrease to low values at deeper stations (Fig. 3f). $H_2S$ produced by sulfate reduction only occurs in deeper parts of sediment cores from the OMZ (Fig. 5b). $H_2S$ formed due to high SRR is reoxidized in the upper centimeters of the OMZ cores, transformed into iron sulfide or, to a minor extent, incorporated into OM (Fig. 5b; Suits and Arthur, 2000). In the deeper parts, however, formation of free $H_2S$ in the pore waters indicates the depletion in the iron-pool reacting with sulfide on short time scales (Canfield et al., 1992; Raiswell and Canfield, 1996). Formation of free $H_2S$ in the pore waters was also reported for shallow Peruvian sediments (Suits and Arthur, 2000) but was not observed in surface upwelling sediments off Chile, except for a shallow harbor site with strong anthropogenic influence (Ferdelman et al., 1997; Zopfi et al., 2000). The sulfur isotopic composition of pyrite ($\delta^{34}S_{pyrite}$) in Peruvian sediments varies significantly with core depth, with minimum and maximum $\delta^{34}S_{pyrite}$ values of −48 and −29‰, respectively (Fig. 5e). These data are within the range of previously published values for upwelling sediments off Chile, sapropels from the Eastern Mediterranean (Passier et al., 1999), and surface sediments of the modern Black Sea (both above and below the chemocline; Table 2). The magnitude of isotope discrimination between sulfate and reduced sulfur species is not affected by reservoir effects (Hartmann and Nielsen, 1969). $\delta^{34}S_{sulfate}$ of

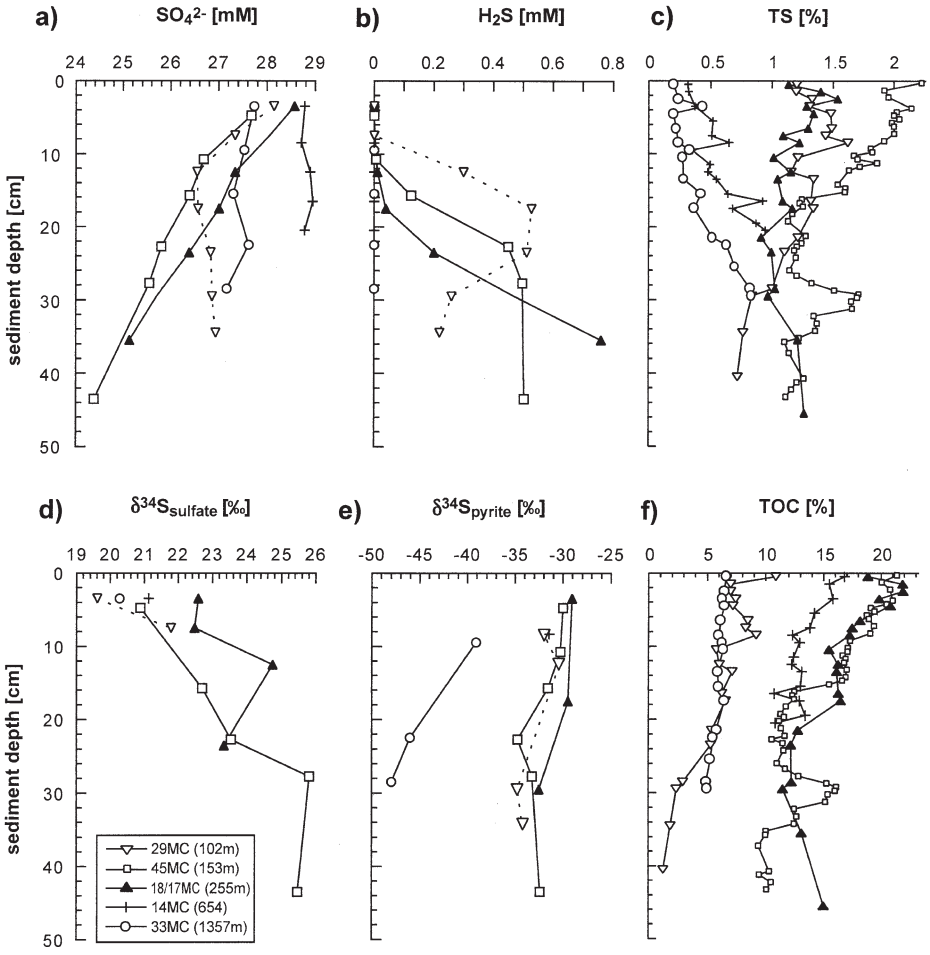


Fig. 5. (a) Downcore profiles of (a) concentration of pore water sulfate, (b) pore water $H_2S$, (c) TS contents, (d) $\delta^{34}S_{sulfate}$ (pore water), (e) $\delta^{34}S_{pyrite}$ (solid phase) and (f) TOC contents for selected cores. TS, TOC data on a carbonate-free basis for 14MC.

modern seawater and in the water column of the upwelling area off Chile is about +21‰ and not affected by element cycling within the OMZ.

A coupling of TS to TOC is indicated by almost parallel downcore profiles for OMZ sediments whereas dissimilar downcore profiles clearly indicate decoupling of TS and TOC for BO sites (Figs. 5c,f). Diminished sulfur isotope fractionation is associated with higher contents of sedimentary TS (Figs. 5c,e). This is due to higher activity of sulfate reducing bacteria when compared to the deep site 33MC. Due to the minor sulfur isotope fractionation during formation of metal sulfides from $H_2S$ solutions (Böttcher et al., 1998; Butler et al., 2000) $\delta^{34}S_{pyrite}$ signatures reflect the $^{34}S/^{32}S$ ratios of $H_2S$ produced during overall sedimentary (sum of microbial and chemical) processes. A comparison of $\delta^{34}S_{pyrite}$ and $\delta^{34}S_{sulfate}$ yields an apparent isotope discrimination of up to −70‰. This fractionation is much higher than results obtained in experiments with pure cultures of sulfate reducing bacteria (e.g., Kaplan and Rittenberg, 1964; Bolliger et al., 2001; Detmers et al., 2001) and was attributed to reactions in the oxidative part of the sulfur cycle such as bacterial disproportionation of sulfur intermediates (Passier et al., 1999; Habicht and Canfield, 2001) and/or sulfate reduction at very low cell-specific rates (Kaplan and Rittenberg, 1964; Wijsman et al., 2001). Bacterial disproportionation of sulfur intermediates leads to an additional $^{34}S$ depletion in the resulting $H_2S$ (Canfield et al., 1998; Cypionka et al., 1998; Habicht et al., 1998; Böttcher et al., 2001).

An increase in accumulation of reactive OM promotes BSR (Berner, 1980). Additionally, rapid burial leads to reservoir-related shifts in net fractionation and moves a given surface sediment layer from the zone of most intense sulfide oxidation where sulfur intermediates are available for disproportionation (with corresponding sulfur isotope effects) into a different diagenetic regime. In agreement with this line of reasoning, the observed overall isotope fractionation decreases with the inferred enhanced activity of sulfate reducing bacteria. This demonstrates the dominant control of isotope discrimination by BSR in the investigated sediments. At lower OM contents, however, an increasing contribution from disproportionation reactions of sulfur species may have to be considered, as indicated by the strong depletion in $^{34}S$ at the deepest station (33MC; Fig. 5e). This is also in agreement with recent findings by Habicht and Canfield (2001) who observed a higher contribution of disproportionation reactions at lower SRR. Furthermore isotope discrimination may be influenced by lower cellular rates, as shown in culture studies by Kaplan and

Table 2. $\delta^{34}S$ of pyrite and pore water sulfate for samples from the Peruvian and Chilean Margin and the NW Black Sea (in brackets = number of analyzed sample; upper 20 cm of sediments).

| Station | Water depth (m) | Range $\delta^{34}S_{pyrite}$ (‰) | Range $\delta^{34}S_{sulfate}$ (‰) | Sampling date |
|---|---|---|---|---|
| Peru Margin[a] | | | | |
| 29MC | 102 | −30.4/−34.8 (4) | 19.6/21.8 (2) | 6-2000 |
| 45MC | 120 | −30.0/−34.7 (6) | 20.9/23.5 (5) | 6-2000 |
| 18MC | 255 | −29.1/−32.5 (3) | 22.5/24.8 (4) | 6-2000 |
| 14MC | 654 | −32.0 (1) | 21.1 (1) | 6-2000 |
| 33MC | 1369 | −39.1/−48.0 (3) | 20.3 (1) | 6-2000 |
| Chile Margin | | | | |
| 4 | 24 | n.d. | 21.7/27.5 (9) | 5-1997 |
| 4[b] | 24 | −27.7/−30.2 (17) | 21.2/22.4 (9) | 5-1998 |
| 7 | 32 | n.d. | 21.2/21.8 (9) | 5-1997 |
| 7[b] | 32 | −32.2/−35.7 | 20.9/21.2 (4) | 5-1998 |
| 7 | 32 | −33.2/−35.3 (2) | 20.6/21.2 (2) | 3-1999 |
| 14 | 64 | n.d. | 21.4/22.7 (16) | 5-1997 |
| 14[b] | 64 | −26.7/−36.4 (15) | 20.8/22.5 (8) | 5-1998 |
| 18 | 88 | −32.0/−38.5 (10) | 21.0/23.9 (12) | 3-1999 |
| 18[b] | 88 | −27.9/−37.2 (7) | 21.1/22.6 (4) | 5-1998 |
| 26 | 122 | n.d. | 21.2/22.5 (9) | 5-1997 |
| NW Black Sea | | | | |
| 2[c] | 26 | −6/−21 (9) | n.d. | 5-1997 |
| 9[c] | 57 | −38/−44 (7) | n.d. | 5-1997 |
| 10[c] | 72 | −42/−46 (4) | n.d. | 5-1997 |
| 24[c] | 137 | −12/−45 (5) | n.d. | 5-1997 |
| St.6 | 394 | −36/−38 (5) | n.d. | 9-1997 |
| 22[c] | 1494 | −37/−40 (7) | n.d. | 5-1997 |

n.d. = not determined.
[a] This study.
[b] Zopfi et al. (2000).
[c] Wijsman et al. (2001).

Rittenberg (1964), or by the changing availability of metabolizable organic compounds which may lead to a different bacterial community structure (Detmers et al., 2001).

The degree of pyritization is visualized in a ternary $Fe_x$-TOC-S diagram (Fig. 6a) which is based on bulk sediment analyses (Brumsack, 1988). The content of reactive iron ($Fe_X$) was estimated empirically assuming that a certain fraction of alumosilicate-bound iron is not available for fast pyrite formation. Canfield et al. (1992) showed that silicate-bound iron only reacts with dissolved sulfide when exposed for very long time periods. Such conditions are not attained in the surface sediments investigated in this study. According to Raiswell and Canfield (1996) 30% of the total iron at the Peru margin consists of a fraction that reacts with sulfide only on time scales of millions of years. Based on an andesitic Fe/Al ratio of 0.48 (see also Fig. 2b) this nonreactive Fe fraction is equivalent to 0.16 multiplied by the Al content.

As shown in Figure 6a many WO samples are TOC-rich and very low in $Fe_X$ and plot below the pyrite saturation line (PSL). This suggests the presence of organic sulfur compounds (Brumsack, 1988), in agreement with extraction results of Suits and Arthur (2000). Most UEO samples are not completely pyritized and approach the PSL. Sediments from BO sites are presumably limited by metabolizable OM. It should be mentioned that a higher proportion of nonreactive Fe would shift samples onto or below the PSL.

At a first glance, Peruvian upwelling sediments exhibit highly variable TOC/TS ratios (Fig. 6b), depending on water depths. UEO site sediments plot close to 'normal marine sediments' which are deposited under oxic conditions (although this classification is defined for max. 5% TOC and 1.8% TS; Berner and Raiswell, 1983). WO site sediments can be discerned into two groups (envelope Fig. 6b). The relatively low TS values (in comparison to TOC) in WO sites result from the lack of Fe available for pyrite formation, the significant sulfide reoxidation (by sulfide-oxidizing bacteria) or loss of free sulfide to the overlying water column. Higher TS values in WO sites also indicate incorporation of sulfur into OM, in agreement with the above reasoning.

### 3.4. Trace Elements

Trace elements may be added to the sediments by preconcentration in, and adsorption to, settling biodetritus, precipitation from solution at the sediment-water interface (SWI), and diffusion to a discrete precipitation depth following a redox gradient. Nameroff et al. (2002), for example, studied metal contents in the water column, sinking particles (sediment traps), and sediments from suboxic sites off Western Mexico and proposed that the direct input of plankton material enriched in metals significantly contributes to the total sedimentary composition, especially for Cd, U, and Mo. Zheng et al. (2000), on the other hand, reported nonlithogenic Mo contents from sinking particles suggesting Mo enrichments with Mn-(hydr)oxides in sediments from the Santa Barbara Basin. In addition, Zheng et al. (2002) state that particulate nonlithogenic U in sinking particles accounts for 10–70% of the total authigenic U in sediments off the central California margin, the Santa Barbara Basin, and Saanich Inlet. Since no sediment trap samples were collected for our study, the role of trace metal

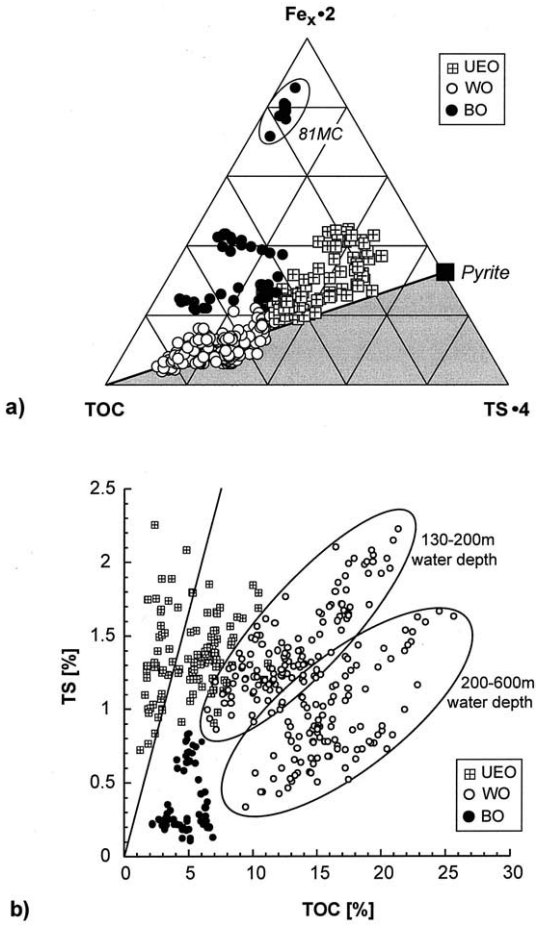


Fig. 6. (a) Major components of Peruvian upwelling sediments in the system $Fe_x \cdot 2\text{-TOC-TS} \cdot 4$ (relative weight ratios); 81MC = glauconite-rich sediments. Grey field indicates sulfur excess and Fe limitation. (b) Scatterplot of TOC vs. TS of all investigated samples (n = 405); line depicts trend for "typical marine sediments" (Berner and Raiswell, 1983). See Figure 3 for symbols.

delivery to the sediments via sinking particles is difficult to assess. Hence, our discussion of TE distribution patterns is as follows: (1) We present TE enrichments vs. lithogenic background and vs. water depth. Downcore TE distribution with special focus on Cd, Mo, Re and Mn reveals insights into their redox-dependent behavior. (2) We discuss anthropogenic metal contributions and present an assessment of mass accumulation rates. (3) We compare TE signatures of upwelling sediments from different areas.

### 3.4.1. Trace Element Distribution with Water Depth and Sediment Depth

As given in the Appendix and shown in Figures 7 and 8, Peruvian upwelling sediments are characterized by extremely high Cd, Mo and Re contents (with enrichment factors, EF $>$ 300 vs. lithogenic background), as well as high Ag, U, Sb, Ni, As (EF $>$ 5), slightly elevated Cr, V, Zn, Cu, Pb, Bi, Tl (EF $>$ 2), and depleted Mn, Co contents (EF $<$ 1). Manganese, Co, Pb, Bi, and Tl contents are highest in sediments from UEO sites decreasing offshore. All other TE contents are most enriched in sediments from WO sites. Cadmium, Mo, and As are least enriched in BO sediments and Re, Ni, U, Sb, Ag, V, Zn, and Cu in UEO sediments. TE depth transect distribution patterns generally follow TOC trends presented in section 3.2.

The good correlation between TS and TOC seen for some samples (section 3.3) simply expresses the sulfide-generating capacity of the diagenetic system (accompanied by good OM preservation) and/or common dilution by lithogenic material. Therefore, one cannot distinguish whether TE (which are known to be trapped with OM and sulfides, like e.g., Mo, Re, Ag, Ni) are primarily associated with TOC or TS in Peruvian samples. Furthermore, incorporation of S species into OM during early diagenesis (section 3.3) and the presence of in situ bacterial biomass additionally hamper the interpretation of TE covariance with TOC and TS. The correlation between TOC (or TS) and TE may reflect direct input of plankton material enriched in TE and preservation.

*3.4.1.1. Mn and Co* The significant depletion in Mn (Fig. 8) implies the loss of Mn by reduction of Mn-(hydr)oxides either in the water column and/or in the reducing sediments. Mobile $Mn^{2+}$ which is produced within the OMZ or within the reducing sediments may be reoxidized in oxygenated waters further offshore, transported in particulate form [$Mn^{4+}$-(hydr)oxides] to the deep ocean floor and accumulated in oxic sediments (e.g., Morford and Emerson, 1999; Schnetger et al., 2000). However, this behavior is not observed in the two deeper water sites ($>$1200 m water depth; Fig. 7). Mn/Al ratios are as low as those within the OMZ, and TOC contents are rather high ($\sim$3–6% TOC) compared to deep-sea sediments (e.g., Arabian Sea, 0.2–0.6% TOC; Schnetger et al., 2000). These observations imply that suboxic conditions must prevail in this depth range, too.

From sediment downcore profiles (Fig. 9a) it becomes further apparent that Mn is depleted vs. the lithogenic background and that Mn/Al ratios are essentially constant or even slightly increase with depth. If significant sedimentary Mn reduction would occur one would expect a near-surface solid-phase Mn peak where bottom water $O_2$ concentrations are higher allowing formation of Mn-(hydr)oxides. However, this is not observed for Peruvian sediments and implies that a significant proportion of Mn-(hydr)oxides was reduced within the suboxic water column before sedimentation.

The behavior of Co provides further indications for the reductive dissolution of Mn-(hydr)oxides. Like Mn, Co is also significantly depleted in Peruvian sediments (Fig. 8) and correlates well with Mn (Fig. 10a). The Mn/Co ratio of Peruvian sediments is identical to the background ratio (Fig. 10a). The behavior of Co strongly parallels that of Mn in seawater (e.g., Bruland, 1983) and in sediments (e.g., Hem, 1989). Co is mobilized in pore waters under suboxic conditions (Heggie and Lewis, 1984) and may diffuse out of the sediments along with Mn (Hartmann, 1964). In contrast to Mn, however, Co is known to form stable sulfides under sulfidic conditions (e.g., Luther, 1991; Huerta-Diaz and Morse, 1992), which are encountered in Peruvian sediments. Burial of Co in the sediments would, therefore, result in lower Mn/Co ratios. However, this is not seen in the samples investigated, leading to the assumption that Mn and Co are mobilized from particles settling through

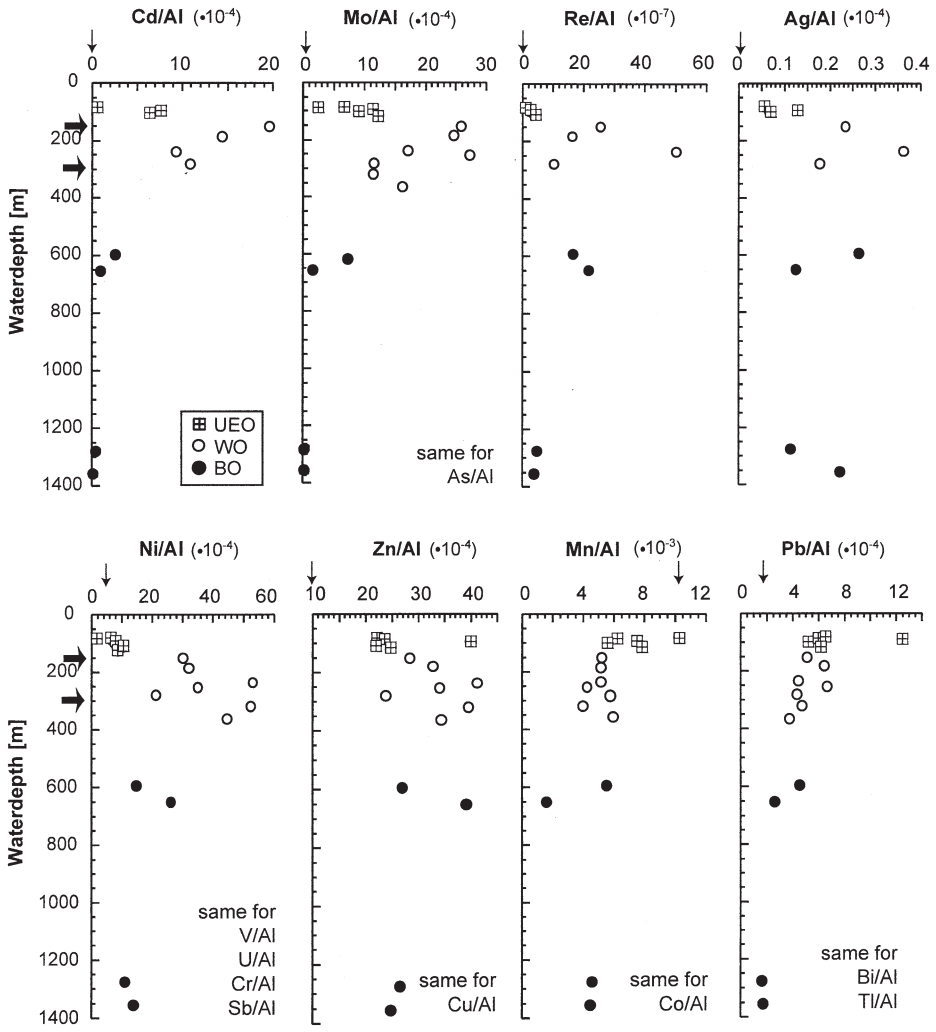


Fig. 7. Waterdepth profile for several trace elements (Al-normalized). Each data point represents the average value (solide phase) for the upper 5 cm of a single investigated core (see Appendix). Vertical arrows indicates lithogenic background. Upper and lower horizontal arrows show TS and TOC maxima, respectively (see Fig. 3 for TS, TOC and symbols).

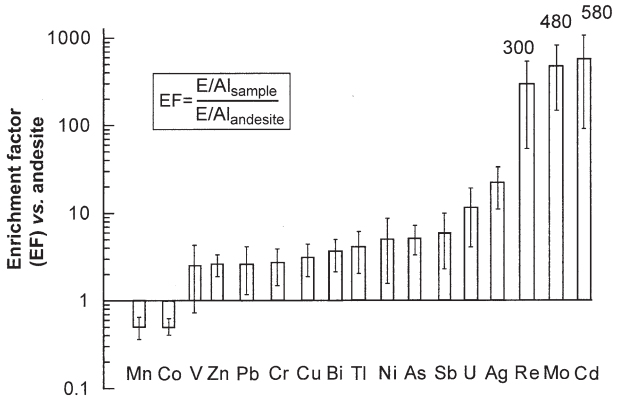


Fig. 8. Enrichment factors for several trace elements vs. average andesitic composition (Sarbas, 2002). Average values from the upper 5 cm of all cores (except turbidites) were used. Ag, Bi, Cd and Tl data from Wedepohl (1971, 1991), Re data from Colodner et al. (1993).

the suboxic water column before reaching the sea floor. Additionally, this process leads to the remobilization of reactive TE scavenged onto Mn-(hydr)oxides. For this reason this carrier phase can be ruled out for TE transport to the WO/BO sediments.

*3.4.1.2. Cd, Mo, and Re* Cadmium is strongly associated with phosphate in the oceans ("nutrient-type element"; Boyle et al., 1976; Bruland, 1983). Phosphoritic deposits accumulate considerable amounts of Cd (e.g., Baturin and Oreshkin, 1984; Nathan et al., 1997). These observations suggest a distinct relationship between Cd and P in biodetritus and sediments. However, our results show that Cd is significantly enriched in sediments with rather low P contents (Fig. 10b). If Cd and P were uniquely derived from productivity Peruvian samples would plot close to the Cd/P ratio of POM ($0.7 \cdot 10^{-3}$; Collier and Edmond, 1984). However, almost all WO and UEO samples plot above this line (Fig. 10b) indicating a preferential P loss (in agreement with findings from section 3.2) relative to Cd. Most BO samples plot along or below this line indicating

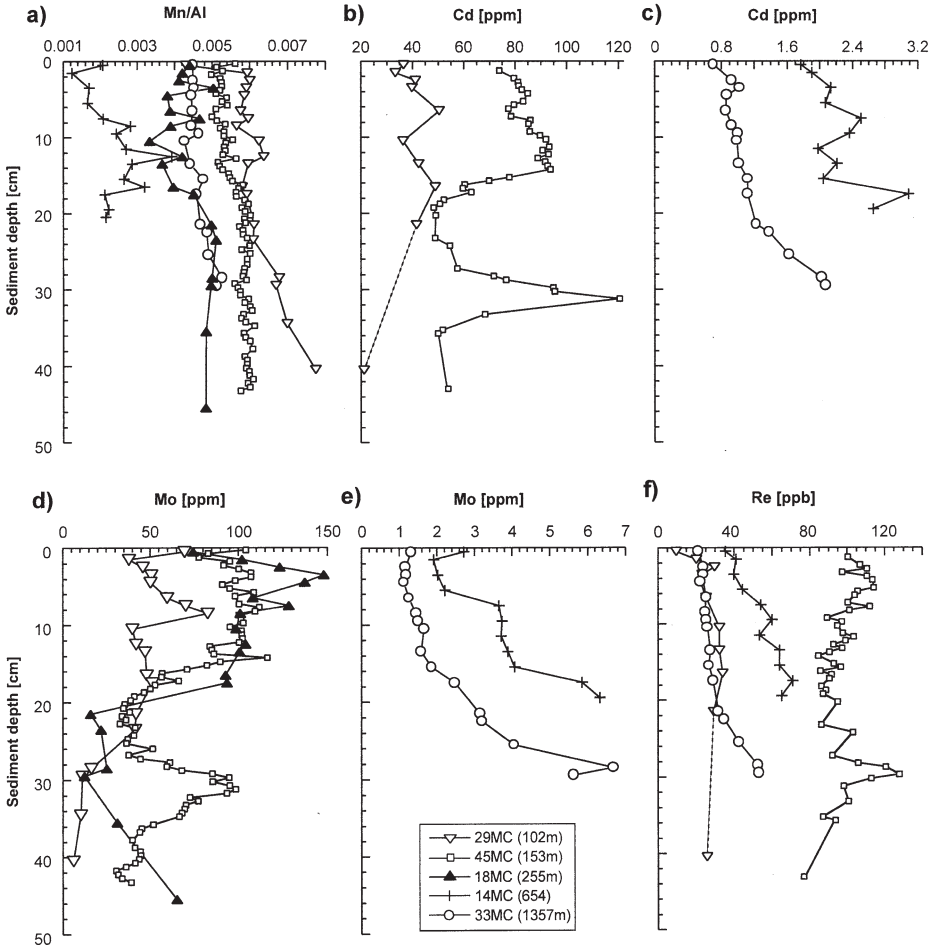


Fig. 9. Downcore profiles of (a) Mn/Al, (b, c) Cd, (d, e) Mo, and (f) Re for selected cores (see also Fig. 5). Al-normalized Cd, Mo, Re (not shown) equal absolute TE contents. Mn was Al-normalized to show depletion vs. background ($Mn/Al_{andesite} = 0.01$). Strong variations in deeper parts of 45MC (b, d) due to lithogical changes, and in upper cm of the cores due to reworking or bioturbation during El Niño (Kriete et al., 2004).

the preferential loss of Cd due to a reduced preservation. Additionally, leaching experiments for Peruvian samples indicate that phosphoritic nodules do not contain significant Cd compared to OM fractions.

The extreme Cd enrichment in contrast to many other TE (Fig. 8) may be due to the distinct metal contribution by plankton (e.g., Collier and Edmond, 1984), strongly inhibited water column regeneration processes owing to shallow water depths and high SR, and efficient sulfide precipitation in the sediments even at trace amounts of $H_2S$ (Rosenthal et al., 1995).

TS contents, Cd/Al and Mo/Al are highest in sediments from sites of less than 300 m water depth and show the same trend (Fig. 7). Moreover, SRR are highest in sediments from sites of ~200 m water depth (Fig. 3f) and show a subsurface peak at 5cm sediment depth. These findings strongly suggest that the presence of $H_2S$ due to near surface SRR seems to be the key process for Cd and Mo accumulation. The good correlation of Mo and Cd (Fig. 10c) suggests (i) similar source and/or (ii) similar mechanism of preservation. But what is the reason for the very high Mo accumulation? To answer this question one has to elucidate the removal pathway of Mo. In the simplest case, Mo diffuses into the sediment pore waters along a concentration and redox gradient from bottom waters to precipitation depth (Shaw et al., 1990; Emerson and Huested 1991). This depth seems to be close to the SWI for anoxic OMZ sediments due to the subsurface sulfate reduction peak (chapter 3.3.) and at deeper depth intervals for suboxic BO sediments (Fig. 9). For the reduction of Mo strongly anoxic (sulfidic) conditions are required (e.g., Emerson and Huested, 1991). However, Helz et al. (1996) hypothesized that in the presence of free $H_2S$, sulfur replaces oxygen on $MoO_4^{2-}$, creating a thiomolybdate complex that promotes Mo scavenging by Fe-S phases and humic materials. This mechanism de-emphasizes the importance of Mo reduction as the initial step in its precipitation under reducing conditions. An anoxic water column was proposed for high Mo removal rates from solution and accumulation in various anoxic basin settings such as the Black Sea or the Mediterranean Sea during sapropel formation (e.g., Emerson and Huested, 1991; Nijenhuis et al., 1998). However, off Peru the water column is suboxic (no $H_2S$) and shows no Mo removal as indicated by dissolved Mo concentrations which equal open ocean values.

From downcore profiles (Figs. 9b–d) it becomes apparent

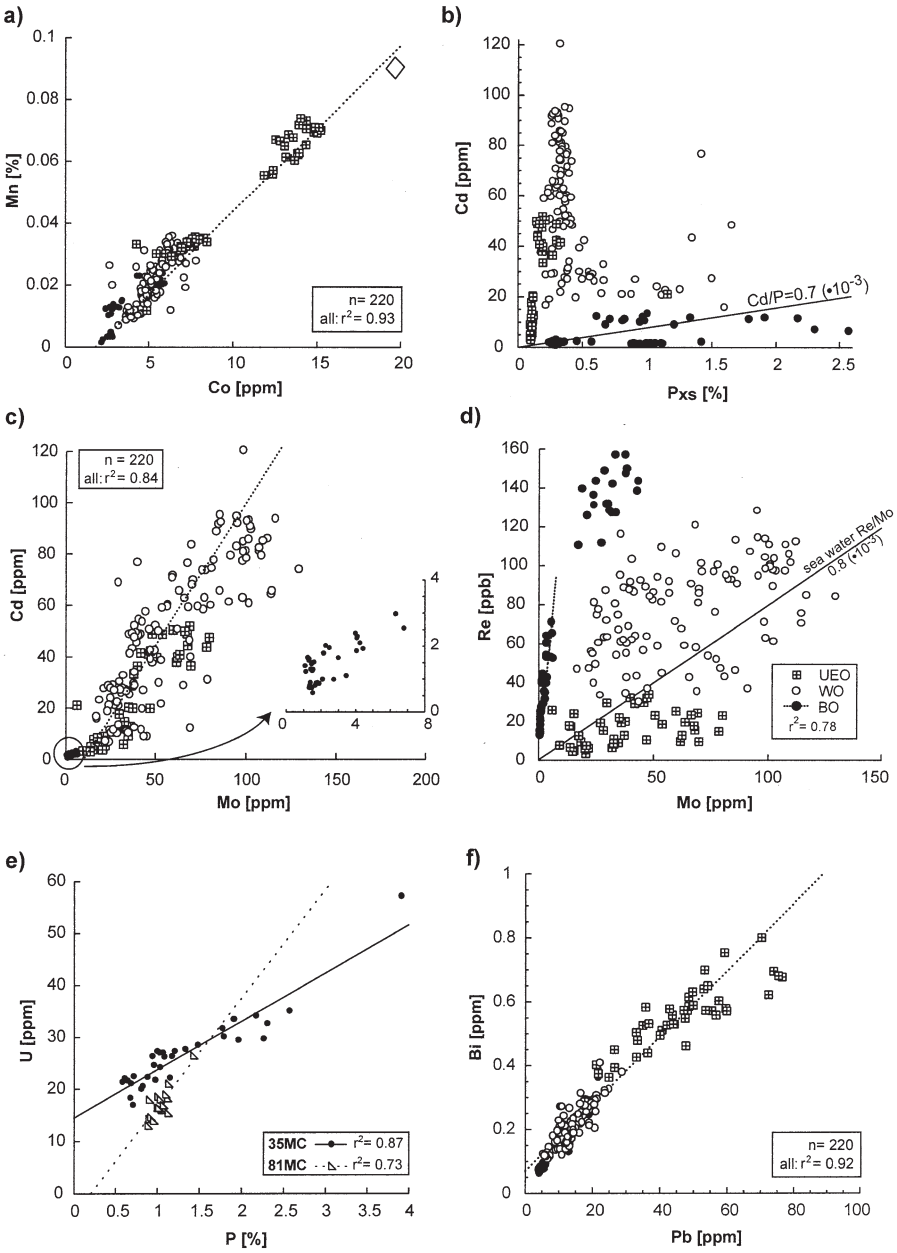


Fig. 10. Scatter plots of (a) Mn vs. Co (diamond = andesite), (b) Cd vs. $P_{xs}$ (Excess P to remove inorganic P, see Fig. 4) (c) Cd vs. Mo for all samples; data from samples from below OMZ are highlighted), (d) Re vs. Mo for all investigated samples (positive correlation exists for samples from below OMZ [except 35MC: isolated cluster; see text]), (e) U vs. P in BO cores (35MC, 81MC), and (f) Bi vs. Pb. For symbols see Figure 3 (except (e)).

that Cd and Mo generally decrease with depth for OMZ sediments whereas they increase with depth for BO sediments. These findings suggest that Cd and Mo removal seems to be governed for BO sediments by diffusion following a redox gradient to precipitation depth as sulfides (see Fig. 5c and Figs. 9c,e). The enrichment with depth in BO sediments is only moderate for Cd whereas it is higher for Mo. This may reflect the higher TE availibility in sea water for Mo than for Cd (e.g., Bruland, 1983). For OMZ sites an authigenic Mo contribution may be important (presumably as a scavenged Mo-phase, as proposed by Helz et al., 1996).

Rhenium is regarded as a paleoredox-indicator element as its concentration is extremely low in the continental crust (0.5 ppb; Crusius et al., 1996) and in oxic sediments (<0.1 ppb; Koide et al., 1986), whereas it may be accumulated to high levels under reducing conditions (Koide et al., 1986; Colodner et al., 1993; Crusius et al., 1996). Rhenium is thought to behave similarly to Mo, with the exception that Mo, in contrast to Re, is rapidly scavenged by Mn-(hydr)oxides (Koide et al., 1986). Rhenium apparently requires suboxic conditions for its removal from solution whereas Mo is accumulating under anoxic (sulfidic) conditions (e.g., Crusius et al., 1996). However, the removal

pathway of Re is poorly understood (it may diffuse across the SWI to precipitation depth; Colodner et al., 1993), and the role of Re contribution by sinking particles is not well constrained.

Rhenium contents increases downcore, even for the UEO site (Fig. 9f). By contrast, Mo decreases downcore at this site. This indicates independent removal pathways for both, Re and Mo for the UEO site. This fact is also indicated by highly variable Re/Mo ratios (Fig. 10d) for WO and UEO sediments. However, the positive correlation of Re and Mo in suboxic BO sediments (Fig. 10d) leads to the assumption that the accumulation of both Re and Mo may be governed by diffusion into the sediments and subsequent fixation most likely as sulfides as indicated by TS contents (Fig. 5c). The high Re/Mo ratios from BO sites (average Re/Mo ratio of 15) indicate suboxic conditions whereas low ratios from WO and UEO sites (close to seawater ratio of $0.8 \cdot 10^{-3}$; Crusius et al., 1996) indicate anoxic conditions.

The very low Re/Mo ratios in UEO site sediments (Fig. 10d) below the seawater ratio are close to the crustal ratio ($0.3 \cdot 10^{-3}$; Crusius et al., 1996). However, the crustal ratio implies oxic depositional conditions (see below) which are definitely not encountered for UEO sites because of high TOC flux/preservation. This contradiction may be explained by (1) an enrichment of Mo relative to Re, and/or (2) a depletion of Re relative to Mo. In case (1) Mo is adsorbed onto Mn-(hydr)oxides that are not reduced when settling through the relatively shallow water column because of high SR. In case (2) the suboxic water column is not reducing enough to account for significant transfer of Re to the sediments, especially when the upper 200 m of the water column turn completely oxic during El Niño events (Levin et al., 2002). This may also have affected the preferential remobilization of more labile Re phases (relative to Mo) which are not yet fixed as sulfides.

*3.4.1.3. Silver* In the oceans, Ag is associated with siliceous material (Martin et al., 1983; Flegal et al., 1995) possibly in the hard parts of diatoms (Fisher and Wente, 1993; Flegal et al., 1995). McKay and Pedersen (2000, 2002) suggest that Ag scavenging onto settling particles delivers Ag to the sediments and/or that the Ag bottom water concentration controls sedimentary Ag enrichment rather than redox conditions. However, the removal mechanism for Ag from seawater is poorly understood.

In samples with low opal contents (almost exclusively samples from BO sites, see Fig. 11a) a good correlation of Ag with opal is observed. In samples with higher opal contents (UEO/WO sites) we observe a good correlation of Ag with TOC (Fig. 11b). However, since TOC and TS are correlated in some samples from WO/UEO sites (section 3.3) an association of Ag with sulfides is also likely for samples presented in Figure 11b. From the above observations we conclude that the source of Ag is diatomaceous matter. For 'low-opal sediments' (Fig. 11a) the original opal/Ag relationship may reflect dissolution processes during particle settling through the deep water column where opal and associated Ag may be remineralized in equal proportions (because Ag can not be trapped). Within fast-accumulating 'high-opal sediments' an early-diagenetic fixation of Ag with OM (or TS) during sedimentary opal dissolution seems likely. Hence, the use of Ag as a proxy for

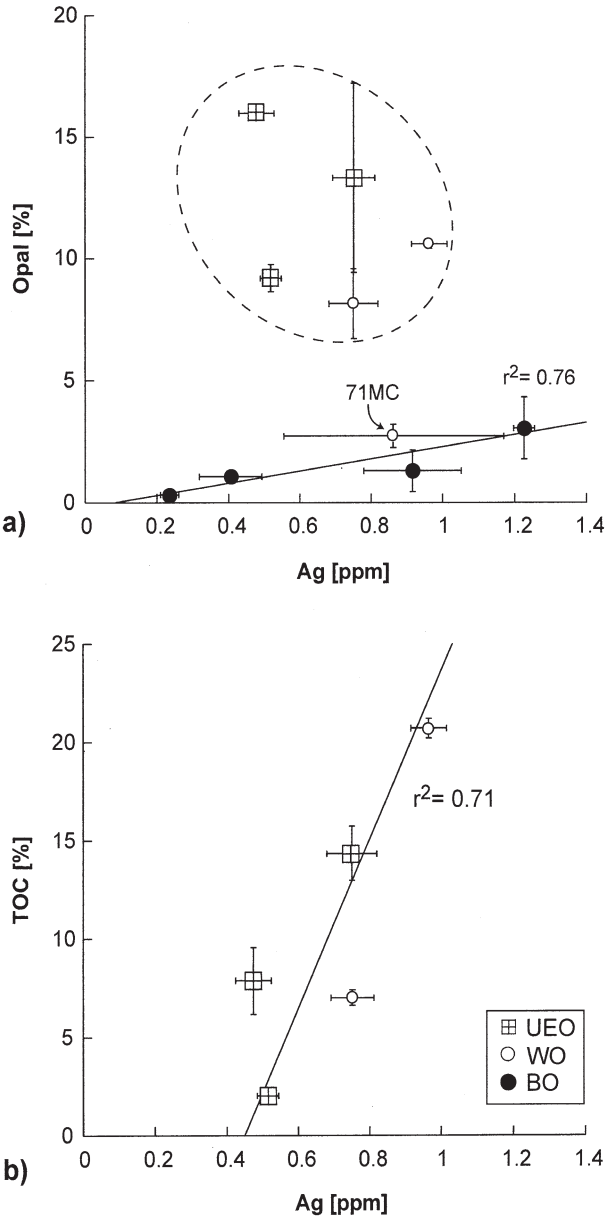


Fig. 11. Scatterplot of Ag vs. (a) opal and (b) TOC. Data are average values (see Appendix). Samples from the envelope in (a) are excluded from curve fit and shown in (b). See Figure 3 for symbols. Opal data (0–2 cmbsf) from Wolf (2002).

paleo-opal flux is questionable because of interfering early-diagenetic processes in response to OM remineralization, like near-surface $H_2S$ generation.

*3.4.1.4. Ni, Zn, Cu, Cr, U and V* Nickel, Zn (and Cu) exhibit a nutrient-type oceanic distribution and display considerable contents in plankton/sinking particles (Broecker 1974; Collier and Edmond 1984). Copper is strongly involved in particle scavenging (Boyle et al., 1977). In reducing environments they may be fixed as sulfides during OM diagenesis (e.g., Kremling, 1983; Huerta-Diaz and Morse, 1992). Uranium, Cr, and V, despite a small depletion in surface waters, are essen-

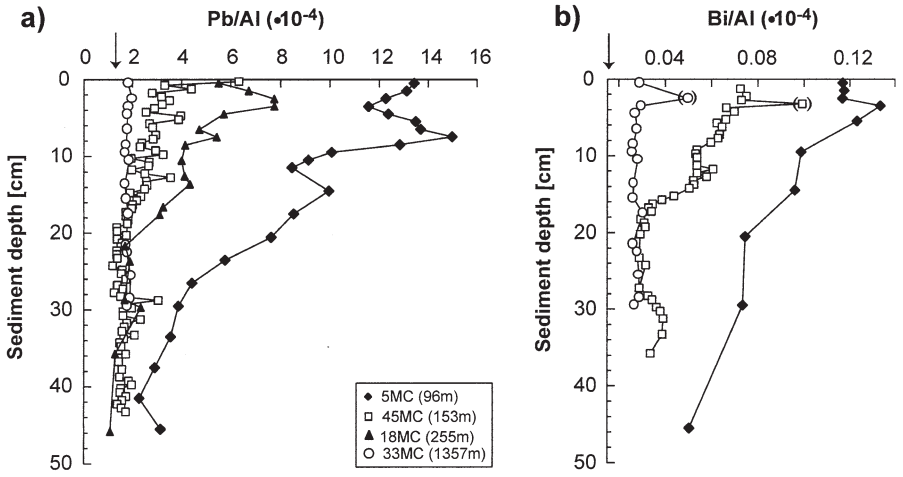


Fig. 12. Depth profiles of (a) Pb/Al and (b) Bi/Al for selected cores. Vertical arrows = lithogenic background. See also Table 3.

tially conservative in oxic waters (e.g., Bruland, 1983) and diffuse into reducing sediments to precipitation depth (e.g., Veeh, 1967; Breit and Wanty, 1991). Uranium and V do not form stable sulfides, however, free sulfide may promote reduction/fixation of both elements (Emerson and Huested, 1991; Klinkhammer and Palmer, 1991). Reduced U is reactive towards organic particles (Kremling, 1983; Calvert et al., 1985; Anderson et al., 1989) and may be removed with OM, as may be the case for Peruvian sediments. However, the good correlation between U and P in two BO cores (Fig. 10e) suggests the early diagenetic enrichment of U with phosphorites, as observed by e.g., Calvert and Price (1983) for upwelling sediments off Namibia. The rather low enrichment in V, Cr, Zn, Ni, Cu (Fig. 8) may result from the masking of the nonlithogenic component by rather high lithogenic metal concentrations. Relatively low Cr, Ni, Cu, and Zn enrichments are also reported for reducing sediments from the Gulf of California (Brumsack, 1989), whereas off Namibia these four metals are moderately enriched because of lower lithogenic metal dilution.

*3.4.1.5. As, Sb, and Tl* Arsenic and Sb occur as (hydr)oxoanions in oxygenated seawater (e.g., Bruland, 1983), and may diffuse into reducing sediments to precipitation depth (Kremling, 1983; Calvert et al., 1985; Huerta-Diaz and Morse, 1992; Thomson et al., 1995). Arsenic shows some nutrient-like distribution in the oceans while Sb appears to be scavenged on metal oxides (Cutter et al., 2001, and refernces therein).

The fixation of As as a sulfide is suggested due to the sulfidic nature of Peruvian sediments (Mossmann et al., 1991; Suits and Arthur, 2000), its distribution pattern similar to Mo (Fig. 7) and the affinity of As to pyrites (Huerta-Diaz and Morse, 1992). However, it remains questionable whether Sb is trapped as a sulfide or in association with OM since highest Sb/Al ratios coincide with the TOC maximum (Fig. 7).

Thallium was thought to belong to the conservative element group in oxic seawater (Flegal and Patterson, 1985). Flegal et al. (1986) suggested that biological activity may be of importance for T1 export to the deep ocean. The likely involvement of T1 in bio-cycling is indicated by recent measurements of T1 in a sea water profile exhibiting a significant surface water depletion in total dissolved T1 and elevated contents of biomethylated T1 (Schedlbauer and Heumann, 2000). However, to date the behavior of T1 under reducing conditions and its mechanism of accumulation is essentially unknown.

The average T1 contents of Peruvian sediments (see Appendix) are lower than those found in other reducing sediments (3–4 ppm T1 on average; Brumsack, 1980; Thomson et al., 1995; Warning and Brumsack, 2000; Lipinski et al., 2003). The involvement of T1 in bio-cycling (Schedlbauer and Heumann, 2000) implies input of T1 through settling biodetritus. The high sulfur contents and the proposed affinity of reduced T1 to pyrite (Heinrichs et al., 1980) suggest trapping of T1 with sulfides in Peruvian sediments.

*3.4.1.6. Pb and Bi* In seawater, Pb and Bi have a low abundance, very short residence times, and are rapidly scavenged (Schaule and Patterson, 1981; Lee et al., 1986). Heinrichs et al. (1980) found Bi enrichments related to TS contents (rather than OM) in black shales with high Cd and Tl contents. In C/T black shales Bi is not significantly enriched compared to adjacent sediments (Brumsack, 1980). Bi is moderately enriched in Mediterranean sapropels (Warning and Brumsack,

Table 3. Assessment of sedimentation rates (SR) for selected cores (see text for details).

| Core | 29MC | 45MC | 18MC | 14MC | 33MC |
|---|---|---|---|---|---|
| Water depth | 102 | 153 | 255 | 654 | 1357 |
| Average core depth (cm) for 1900 A.D.[a] | 30 | 18 | 20 | —[b] | —[b] |
| Estimated avg. SR [cm/kyr] | 300 | 180 | 200 | 100[c] | 100[c] |

[a] Onset of anthropogenic Pb contribution to sediments.
[b] No visible Pb enrichment above average andesite.
[c] Assumed according to comparable data from Levin et al. (2002).

Table 4. $\delta^{34}S$ (pyrite), dry weight density ($\rho_{dry}$) and contents and accumulation rates (AR) for TOC and Re/Mo for selected samples; see Eqn. 1 for calculations (14MC: TOC on a carbonate-free basis).

| Core | Depth (cm) | $\delta^{34}S_{pyr}$ (‰) | $\rho_{dry}$ (g cm$^{-3}$) | TOC (%) | AR TOC (g cm$^{-2}$ kyr) | Re/Mo ($\times 10^{-3}$) |
|---|---|---|---|---|---|---|
| 29MC | 12.5 | −30.4 | 1.70 | 6.03 | 30.7 | 0.60 |
| | 29.5 | −34.8 | 2.50 | 2.38 | 17.8 | 2.24 |
| | 34.5 | −34.2 | 3.20 | 1.86 | 17.9 | 2.30 |
| 45MC | 4.75 | −30.0 | 1.34 | 19.1 | 46.1 | 1.10 |
| | 10.75 | −30.3 | 1.32 | 17.1 | 40.1 | 0.63 |
| | 15.75 | −31.6 | 1.75 | 14.0 | 44.1 | 1.36 |
| | 22.75 | −34.7 | 1.97 | 10.5 | 37.3 | 2.89 |
| | 27.75 | −33.2 | 1.40 | 12.8 | 32.4 | 1.54 |
| | 43.5 | −32.4 | 1.70 | 10.0 | 30.6 | 1.74 |
| 18MC | 3.5 | −29.1 | 1.10 | 19.8 | 43.6 | 0.75 |
| | 17.5 | −29.5 | 1.15 | 16.5 | 38.0 | 0.90 |
| | 29.5 | −32.5 | 2.00 | 11.5 | 45.9 | 2.52 |
| 14MC | 8.5 | −32.0 | 2.19 | 12.2 | 26.8 | 15.4 |
| 33MC | 9.5 | −39.1 | 2.14 | 6.29 | 13.4 | 16.9 |
| | 22.5 | −46.0 | 2.10 | 5.50 | 11.5 | 10.9 |
| | 28.5 | −48.0 | 1.97 | 4.90 | 9.65 | 7.84 |

2000) and Jurassic/Cretacecous black shales from the Norwegian shelf (Lipinski et al., 2003).

Lead and Bi are enriched vs. lithogenic levels in Peruvian UEO near-surface sediments (Figs. 7 and 8) and correlate well (Fig. 10f). The enrichment patterns of Pb and Bi (Fig. 7) suggest an offshore decreasing anthropogenic contribution, rapid scavenging and removal from solution, in agreement with findings of Schaule and Patterson (1981) and Lee et al. (1986). The proposed anthropogenic contribution of Pb (Bi) to the sediments is further evidenced by shallow enrichments (up to 10 times) over the lithogenic background (Fig. 12). The variation seen in the upper cm of some profiles (Fig. 12) may result from bioturbation or resuspension processes most likely during periods of bottom water ventilation.

SR may be estimated from the onset of the near-surface Pb anomaly. Previous work showed that SR are generally high on the Peruvian shelf decreasing offshore with local variations depending on the position of upwelling cells, clastic riverine supply and current strengths all influencing the distribution of sinking particles (e.g., Reimers and Suess, 1983; McCaffrey et al., 1990; Levin et al., 2002; Kriete et al., 2004).

Lead forms a major constituent in mineral deposits from the Andes (like porphyry copper deposits; e.g., MacFarlane et al., 1990). In association with these deposits high contents of Bi are commonly reported (Vila et al., 1991; Sillitoe, 2003). According to Benavides (1990) the mining industry in Peru started to prosper at the end of the 19th century. If the onset of anthropogenic Pb at around 30 cm core depth for site 5MC (Fig. 12a) corresponds to the year 1900, we obtain a linear sedimentation rate (LSR) of 0.3 cm · yr$^{-1}$ which is in agreement with SR for 5MC reported by Kriete et al. (2004) using $^{210}$Pb and $^{137}$Cs measurements. LSR can be estimated for other cores simply by establishing the onset of the anthropogenic Pb contribution using the downcore Pb/Al profile (Fig. 12; results in Table 3).

Given the assumed sedimentation rates (Table 3) and measured bulk dry density ($\rho_{dry}$; Table 4) for the five cores discussed in chapter 3.3, accumulation rates (AR) can be calculated for TOC according to the following equation:

$$AR_{TOC} = TOC \cdot SR \cdot \rho_{dry} \quad (1)$$

From Figures 13a,b it is apparent that $\delta^{34}S_{pyrite}$ is positively

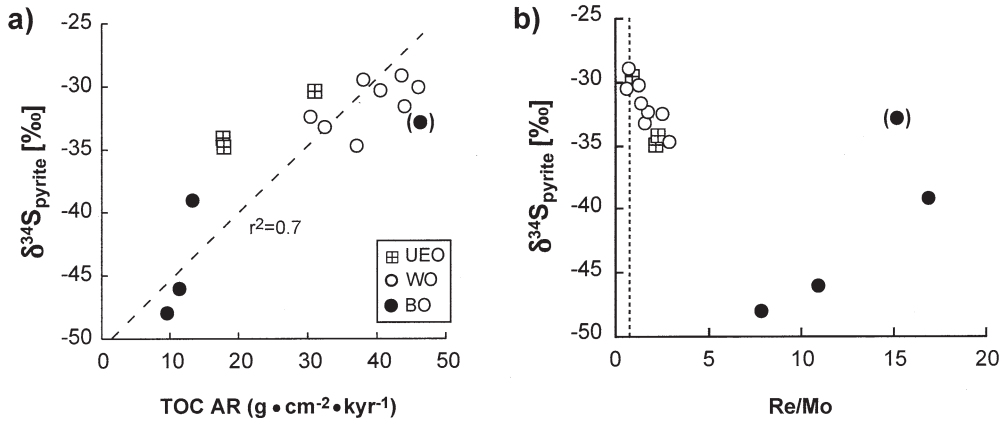


Fig. 13. $\delta^{34}S_{pyrite}$ values vs. (a) accumulation rates of TOC and (b) Re/Mo for selected samples of this study (see also Table 4). Data point for 14MC (reworked carbonate sediments) in brackets excluded from curve fit calculation. Vertical dashed line = seawater ratio. See Figure 3 for symbols.

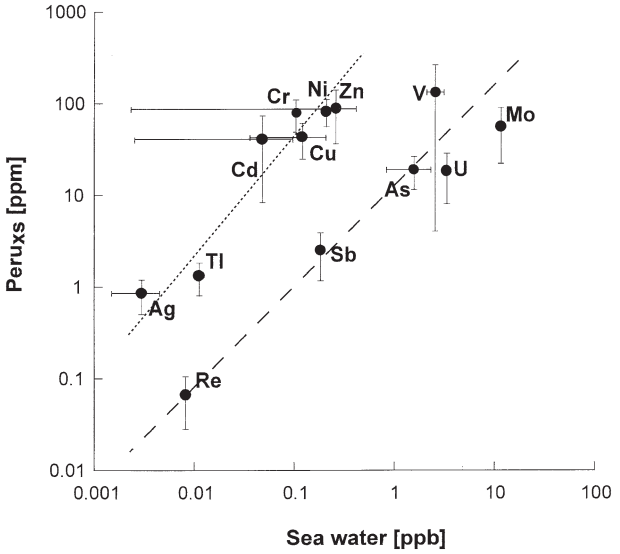


Fig. 14. Scatter plot of average TE concentration in sea water vs. $TE_{xs}$ contents (average of the upper 20cm) from Peruvian sediments ($Peru_{XS}$). For calculation of excess contents see Figure 4. Samples with higher Zr/Al ratios ($>30 \cdot 10^{-4}$) (and therefore many samples from suboxic BO sites) were excluded from calculation. Sea water TE data from Bruland (1983) and references in Morford and Emerson (1999). See text for details.

correlated with $AR_{TOC}$ and negatively correlated with Re/Mo ratios (indicative for overall sedimentary redox conditions). This indicates that sulfur isotope fractionation and disproportionation of sulfur intermediates increase when $AR_{TOC}$ decrease and overall sedimentary redox conditions become less reducing.

### 3.4.2. *Metal Accumulation in Peruvian Sediments and Metal Abundance in Seawater*

The significant TE enrichment seen in Peruvian upwelling sediments raises the question of metal sources. Any sedimentary excess metal content must be related to metal availability in seawater or metal preconcentration in marine plankton/particles and associated preservation processes. To test this hypothesis we have plotted average excess TE contents of Peruvian upwelling sediments vs. seawater concentrations for various TE investigated (Fig. 14). Two differing trends are seen: Re, Sb, As, U, Mo and V enrichment seems to be directly related to seawater TE availability. We interpret this as TE accumulation by fixation processes from seawater diffusing to precipitation depth, either as sulfides or bound (possibly in a reduced state) to OM. The depth of free $H_2S$ appearance in the sedimentary column is a critical factor for the degree of enrichment of these TE.

Another group of elements including Cd, Cu, Zn, Ni, Cr, Ag, and T1 plots two orders of magnitude above the seawater trend. These elements are involved in nutrient-type bio-cycling processes and characterized by surface-seawater depletion (see compilation in Bruland, 1983; Schedlbauer and Heumann, 2000). At the same time most of these TE are enriched in plankton (see Brumsack, 1986 and references therein). Hence, this group of elements is brought to the sediments by biodetritus. The close vicinity of $H_2S$ at the SWI plays an important role in preventing metal regeneration thus fostering TE fixation. Figure 14 therefore clearly demonstrates, that TE patterns in Peruvian upwelling sediments bear a close relationship to TE behavior and availability in seawater.

### 3.4.3. *Comparison of Peruvian Upwelling Sediments with Those from Other Areas*

Upwelling areas such as the Gulf of California (GOC), the Arabian Sea and the Namibian Margin are characterized by high primary production and subsequent formation of an intense OMZ (see Table 5). Sediments deposited beneath upwelling areas are known to accumulate several TE under suboxic or anoxic conditions. In the following, accumulation rates for Peruvian TE and TOC data are compared with data compiled from the literature. TE data are expressed as excess contents (see Fig. 4 for calculation), since the proportion of diluting lithogenic material (as reflected by total Al contents) varies strongly from area to area. High energy sediments (characterized by higher Zr/Al ratios $>30 \cdot 10^{-4}$) were excluded from calculating average values for Peruvian sediments. In Figure 15 average TE excess and TOC AR are compared with those from the Gulf of California (GOC; Brumsack, 1989), Oman Margin (Morford and Emerson, 1999) and Namibian Margin. All sediments are comparable in lithology and consist of diatomaceous to diatom bearing mud (with minor contents of carbonate and silt). Unfortunately, element data are incomplete (see below) and the number of cores investigated is lower for the other upwelling areas.

Five short cores from 400–800 m water depth (within OMZ) presented by Brumsack (1989) were taken from the eastern slope of the GOC. The short core recovered off Namibia during Meteor cruise M48–2 (Emeis, 2000) was taken from 83 m water depth within the strong OMZ that occasionally experiences $H_2S$ eruptions from underlying sediments (Hart and Currie, 1960). Morford and Emerson (1999) presented TE data for Cd, Mo, Mn, Re, V, U from three cores recovered off Oman from a transect through the OMZ. For this comparison, only data from core TN047–20 (806 m water depth, OMZ) were used since at this location bottom water $O_2$ concentration was below detection limit and TE enrichment was highest (Morford and Emerson, 1999). TOC values from Pedersen et al. (1992) were used from comparable water depths and geographical position.

Peruvian upwelling sediments show highest enrichments for TOC, Cd, Mo, U, and V, followed by Namibian upwelling sediments. These two settings strongly contrast the low TOC and TE abundance in sediments from the GOC and Oman margin (Fig. 15). For Peru and Namibia, the combination of perennial upwelling, high productivity, a strong OMZ, and strong sulfate reduction along with free $H_2S$ close to the SWI seem to promote OM and TE preservation.

The OM preservation encountered throughout the Oman margin is diminished due to efficient sediment reworking by bottom currents and subsequent OM degradation (Pedersen et al., 1992). Moreover, sulfate reduction (Passier et al., 1997) and the formation of pyrite (Schenau et al., 2002) is less intense, lowering the TE fixation capacity. Additionally, a strong sea-

Table 5. Basic characteristics of different upwelling systems.

| Site | Upwelling type | OMZ (m water depth) | Avg. prim. production (g C $m^{-2}yr^{-1}$) | Avg. sed. rates (cm $kyr^{-1}$)[a] |
|---|---|---|---|---|
| Peru | year-round[b] | 50-650[f] | 350[h] | 150[i] |
| Oman | seasonal[c] | 150-1200[c] | 300[c] | 14[c] |
| Gulf of California | seasonal[d] | 400-800[d] | 100[d] | 180[d] |
| Namibia | year-round[e] | 50-700[g] | 300[e] | 100[e] |

[a] Within OMZ.
[b] De Mendiola (1981).
[c] References in Morford and Emerson (1999).
[d] References in Brumsack (1989).
[e] Calvert and Price (1983) and references therein.
[f] Lückge and Reinhardt (2000); Emeis et al. (1991).
[g] Emeis (2000).
[h] Müller and Suess (1979).
[i] Reimers and Suess (1983); McCaffrey et al. (1990); Kriete et al. (2004); Levin et al. (2002); this work.

sonality and a comparably low AR hamper efficient input of productivity-derived TE.

For the eastern slope of the GOC, fresh OM is produced and exported during the dry winter season whereas terrigenous detrital material is deposited during the wet summer (Brumsack, 1989, and references therein). Brumsack and Gieskes (1983) reported that BSR is intense and that reducing conditions promote TE accumulation (Brumsack, 1989). However, lower TE accumulation may be influenced by (a) lower primary production rates (subsequently lower biologic uptake of nutrient-type TE; Table 5), (b) strong upwelling seasonality (affecting the dimensions of the OMZ), and (c) iron availability and ongoing pyritization at greater sediment depth. Therefore, enhanced productivity and a strong OMZ alone do not lead to significant TE accumulation off Oman and in the GOC.

## 4. CONCLUSIONS

This study presents results of an extended geochemical study on Peruvian near-surface upwelling sediments. The most important facts are summarized in the following and visualized in a general scheme (Fig. 16).

(1) High TOC contents within OMZ sediments are due to enhanced preservation whereas P is preferentially remineralized within OMZ sediments (no P trapping with Fe-(hydr)oxides) and only enriched in phosphorites in sediments below the OMZ. High opal contents in the sediments decreasing offshore reflect high near-shore diatom productivity off Peru whereas biogenic carbonate contents and Zr/Al ratios increase offshore indicating calcareous plankton production and/or current influences on sediment deposition.

(2) Intense sulfur cycling at the sediment-water interface is indicated by strong depletions of $^{34}S$ in sedimentary pyrite. $\delta^{34}S$ values as light as $-48‰$ indicate isotope fractionation relative to sea water sulfate by BSR. Such low $\delta^{34}S$ values are most likely explained by additional sulfide reoxidation and disproportionation of sulfur intermediates when overall sedimentary redox conditions become less reducing and AR decrease. In all cores the highest SRR were observed in the top 5 cm where pore water sulfate concentrations varied little due to resupply of sulfate by sulfide oxidation and/or diffusion of sulfate from bottom water.

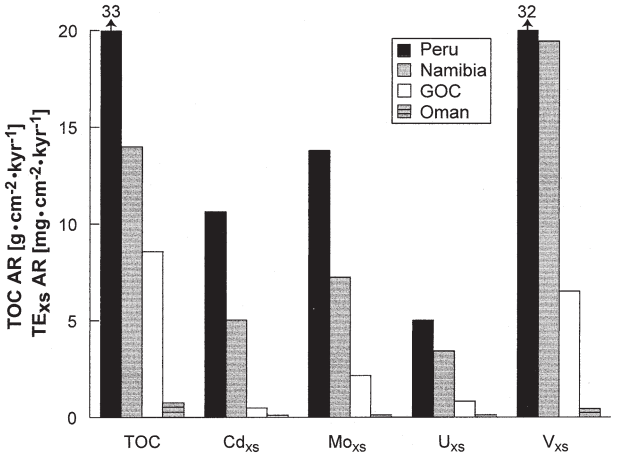


Fig. 15. Comparison of average accumulation rates for excess TE and TOC (average of the upper 20 cm) from Peruvian sediments (this study), Oman Margin (TE data: Morford and Emerson, 1999; TOC data: Pedersen et al., 1992), Gulf of California (GOC, Brumsack, 1989) as well as Namibia Margin. See text for details, and Figure 4 for calculation of excess contents. Dry bulk densities were assumed to be $\sim 1.4–1.8\ g \cdot cm^{-3}$ (sediments off Namibia, Oman, Gulf of California).

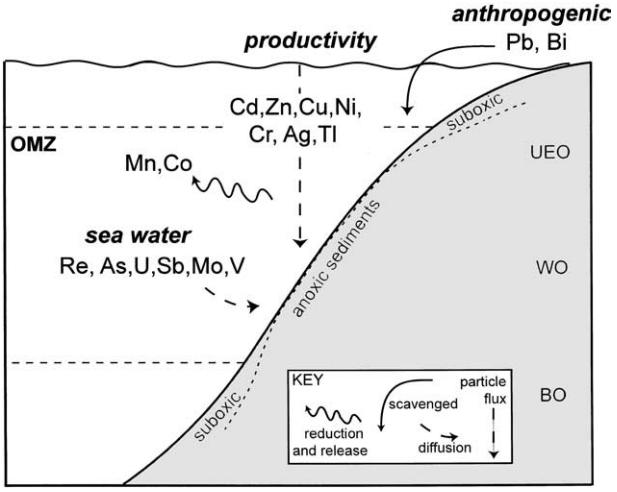


Fig. 16. Scheme summarizing geochemical processes encountered off Peru.

(3) Mn and Co are significantly depleted in WO/BO sediments most likely due to mobilization from particles within the water column when settling through the OMZ. Diffusion of Mn and Co from reducing sediments only seems to occur in near-coastal UEO sediments at shallow sediment depth.

(4) Cadmium, Mo and Re are extremely enriched (with enrichment factors $>$ 300 *vs.* lithogenic background) in WO sediments ($<$600 m water depth). High Re and moderate Cd and Mo enrichments are seen in BO sediments ($>$600 m water depth). Due to their specific behavior under different redox conditions the Re/Mo ratios indicate anoxic conditions for UEO/WO and suboxic conditions for BO sediments. Cadmium is considerably contributed to OMZ sediments by biodetritus.

(5) Silver transfer to 'low-opal' BO sediments bears a distinct relationship to opaline matter input. Within fast-accumulating 'high-opal sediments' an early-diagenetic fixation of Ag with OM (or TS) during sedimentary opal dissolution seems likely. Based on these findings the use of Ag as a proxy for paleo-opal flux is questionable because of interfering early-diagenetic processes in response to OM remineralization.

(6) Uranium is distinctly enriched in WO sediments (due to sulfidic sedimentary conditions) and in some BO sediments (due to formation of phosphorites).

(7) Lead and Bi are contributed by anthropogenic mining activity to coastal sediments, allowing to estimate sediment accumulation rates. $\delta^{34}S_{pyrite}$ is positively (negatively) correlated with $AR_{TOC}$ (Re/Mo ratios), indicating an increase in sulfur isotope fractionation and disproportionation of sulfur intermediates when $AR_{TOC}$ decrease and sedimentary redox conditions become less reducing.

(8) Rhenium, Sb, As, U, Mo, and V enrichment seems to be directly related to seawater TE availability, implying diffusive supply to a certain precipitation depth and fixation either as sulfides or bound to OM. The dominant source for elements like Ag, Cd, Cu, Zn, Ni, Cr, and T1, seems to be biodetritus. The depth of free $H_2S$ appearance in the sedimentary column is a critical factor for the degree of TE enrichment.

(9) TOC, Cd, Mo, U, and V accumulation rates of Peruvian (and Namibian) upwelling sediments by far exceed those from off Oman and the Gulf of California. For Peru (and Namibia), the combination of perennial upwelling, high productivity, a strong OMZ, high SR of OM and high SRR promote OM/TE accumulation.

*Acknowledgments*—We thank the crew of the R/V *Sonne,* O. Dellwig and B. Harazim for onboard sampling, J. Niggemann for fruitful discussions. A. Wolf kindly provided the opal data. Timothy W. Lyons and two anonymous reviewers are thanked for their constructive comments. We greatly acknowledge the financial support from BMBF (03G0147B), DFG (Schn 381/2), and the Max Planck Society.

*Associate editor:* T. Shaw

## REFERENCES

Anderson R. F., LeHuray A. P., Fleisher M. Q., and Murray J. W. (1989) Uranium deposition in Saanich Inlet sediments, Vancouver Island. *Geochim. Cosmochim. Acta* **53,** 2205–2213.

Arthur M. A. and Sageman B. B. (1994) Marine shales: Depositional mechanisms and environments of ancient deposits. *Annu. Rev. Earth Planet. Sci.* **22,** 499–551.

Arthur M. A., Dean W. E., and Laarkamp K. (1998) Organic carbon accumulation and preservation in surface sediments on the Peru margin. *Chem. Geol.* **152** (*3–4*), 273–286.

Atherton M. P. and Sanderson L. M. (1985) The chemical variation and evolution of the superunits of the segmented coastal batholith. In *Magmatism at a Plate Edge—The Peruvian Andes* (eds. W. S. Pitcher, M. P. Atherton, E. J. Cobbing and R. D. Beckinsale), pp. 328. Blackie.

Baturin G. N. and Oreshkin V. N. (1984) Behavior of cadmium in bone phosphate from the ocean-floor. *Geokhimiya* **8,** 1231–1237.

Benavides A. (1990) Exploration and mining ventures in Peru. *Econ. Geol. Bull. Soc. Econ. Geol.* **85** (*7*), 1296–1302.

Berner R. A. (1980) *Early Diagenesis: A Theoretical Approach*. Princeton University Press.

Berner R. A. and Raiswell R. (1983) Burial of organic carbon and pyrite sulfur in sediments over Phanerozoic time: A new theory. *Geochim. Cosmochim. Acta* **47,** 855–862.

Bolliger C., Schroth M. H., Bernasconi S. M., Kleikemper J., and Zeyer J. (2001) Sulfur isotope fractionation during microbial sulfate reduction by toluene-degrading bacteria. *Geochim. Cosmochim. Acta* **65** (*19*), 3289–3298.

Böttcher M. E., Smock A. M., and Cypionka H. (1998) Sulfur isotope fractionation during experimental precipitation of iron(II) and manganese(II) sulfide at room temperature. *Chem. Geol.* **146** (*3–4*), 127–134.

Böttcher M. E., Thamdrup B., and Vennemann T. W. (2001) Oxygen and sulfur isotope fractionation during anaerobic bacterial disproportionation of elemental sulfur. *Geochim. Cosmochim. Acta* **65** (*10*), 1601–1609.

Boyle E. A., Sclater F. R., and Edmond J. M. (1976) Marine geochemistry of cadmium. *Nature* **263** (*5572*), 42–44.

Boyle E. A., Sclater F. R., and Edmond J. M. (1977) The distribution of dissolved copper in the pacific. *Earth Planet. Sci. Lett.* **37** (*1*), 38–54.

Breit G. N. and Wanty R. B. (1991) Vanadium accumulation in carbonaceous rocks: A review of geochemical controls during deposition and diagenesis. *Chem. Geol.* **91,** 83–97.

Brockmann C., Fahrbach E., Huyer A., and Smith R. L. (1980) The poleward undercurrent along the Peru coast—5 degrees S to 15 degrees S. *Deep-Sea Res. A***27** (*10*), 847–856.

Brodie I. and Kemp A. E. S. (1994) Variation in biogenic and detrital fluxes and formation of laminae in Late Quaternary sediments from the Peruvian coastal upwelling zone. *Mar. Geol.* **116** (*3–4*), 385–398.

Brodie I. and Kemp A. E. S. (1995) Pelletal structures in Peruvian upwelling sediments. *J. Geol. Soc.* **152,** 141–150.

Broecker W. S. (1974) *Chemical Oceanography*. Harcourt Brace Jovanovich.

Bruland K. W. (1983) Trace elements in sea-water. In *Chemical Oceanography,* Vol. 8 (eds. J. P. Riley and R. Chester), pp. 157-220. Academic Press.

Brumsack H.-J. (1980) Geochemistry of Cretaceous black shales from the Atlantic Ocean (DSDP Legs 11, 14, 36 and 41). *Chem. Geol.* **31,** 1–25.

Brumsack H.-J. (1986) The inorganic geochemistry of Cretaceous black shales (DSDP Leg 41) in comparison to modern upwelling sediments from the Gulf of California. In *North Atlantic Palaeoceanography* (eds. C. P. Summerhayes and N. J. Shackleton), pp. 447-462. Special Publications 21. Geological Society.

Brumsack H.-J. (1988) Rezente, $C_{org}$-reiche Sedimente als Schlüssel zum Verständnis fossiler Schwarzschiefer. Habilitations-Schrift, Universität Göttingen.

Brumsack H.-J. (1989) Geochemisty of recent TOC-rich sediments from the Gulf of California and the Black Sea. *Geol. Rundschau* **78** (*3*), 851–882.

Brumsack H.-J. and Gieskes J. M. (1983) Interstitial water trace-metal chemistry of laminated sediments from the Gulf of California, Mexico. *Mar. Chem.* **14,** 89–106.

Butler I. B., Böttcher M. E., and Rickard D. (2000) Sulfur isotope discrimination during experimental formation of pyrite. *J. Conf. Abstr.* **5,** 272–273.

Calvert S. E. and Price N. B. (1983) Geochemistry of Namibian shelf sediments. In *Coastal Upwelling—Its Sediment Record, Part A:*

*Response of the Sedimentary Regime to Present Coastal Upwelling,* Vol. 10a (eds. E. Suess and J. Thiede), pp. 337-375. Plenum Press.

Calvert S. E., Mukherjee S., and Morris R. J. (1985) Trace metals in fulvic and humic acids from modern organic-rich sediments. *Oceanol. Acta* **8** (*2*), 167–173.

Canfield D. E. (1994) Factors influencing organic carbon preservation in marine sediments. *Chem. Geol*. **114,** 315–329.

Canfield D. E., Raiswell R., and Bottrell S. (1992) The reactivity of sedimentary iron minerals toward sulfide. *Am. J. Sci.* **292,** 659–683.

Canfield D. E., Thamdrup B., and Fleischer S. (1998) Isotope fractionation and sulfur metabolism by pure and enrichment cultures of elemental sulfur-disproportionating bacteria. *Limnol. Oceanogr.* **43** (*2*), 253–264.

Clapperton C. M. (1993) *Quaternary Geology and Geomorphology of South America.* Elsevier Science.

Collier R. and Edmond J. (1984) The trace element geochemistry of marine biogenic particulate matter. *Progr. Oceanogr.* **13,** 113–199.

Colodner D., Sachs J., Ravizza G., Turekian K., Edmond J., and Boyle E. (1993) The geochemical cycle of rhenium: A reconnaissance. *Earth Planet. Sci. Lett.* **117** (*1–2*), 205–221.

Crusius J., Calvert S., Pedersen T., and Sage D. (1996) Rhenium and molybdenum enrichments in sediments as indicators of oxic, suboxic and sulfidic conditions of depostition. *Earth Planet. Sci. Lett.* **145,** 65–78.

Cutter G. A., Cutter L. S., Featherstone A. M., and Lohrenz S. E. (2001) Antimony and arsenic biogeochemistry in the western Atlantic Ocean. *Deep-Sea Res. II* **48** (*13*), 2895–2915.

Cypionka H., Smock A. M., and Böttcher M. E. (1998) A combined pathway of sulfur compound disproportionation in Desulfovivrio desulfuricans. *FEMS Microbiol. Lett.* **166** (*2*), 181–186.

De Mendiola R. B. (1981) Seasonal phytoplankton distribution along the Peruvian coast. In *Coastal Upwelling* (ed. F. A. Richards), pp. 348-356. American Geophysical Union.

Detmers J., Brüchert V., Habicht K., and Küver J. (2001) Diversity of sulfur isotope fractionation by sulfate-reducing procaryotes. *Appl. Environ. Microbiol.* **76,** 888–894.

Ding T., Valkiers S., Kipphardt H., De Bievre P., Taylor P. D. P., Gonfiantini R., and Krouse R. (2001) Calibrated sulfur isotope abundance ratios of three IAEA sulfur isotope reference materials and V-CDT with a reassessment of the atomic weight of sulfur. *Geochim. Cosmochim. Acta* **65** (*15*), 2433–2437.

Dullo W. C., Rein B., Wolf A., Biebow N., Schaber K. and Sirocko F. (2000) Core descriptions and reflectance spectra. In *Cruise Report SO147 Peru Upwelling: Valparaiso—Callao, 29.05.-03.07.2000* (ed. H. R. Kudrass), pp. 102-119. BGR Hannover.

Emeis K. C. (2000) *Cruise Report Meteor 48–2 (Walvis Bay-Walvis Bay, 5–23 August, 2000) IOW*. Warnemünde, Germany.

Emeis K. C. and Morse J. W. (1990) Organic carbon, reduced sulfur, and iron relationships in sediments of the Peru margin, Sites 680 and 688. In *Proceedings of the Ocean Drilling Program, Scientific Results,* Vol. 112 (eds. E. Suess and R. von Huehne), pp. 441-454. Ocean Drilling Program.

Emeis K. C., Whelan J. K. and Tarafa M. (1991) Sedimentary and geochemical expression of oxic and anoxic conditions on the Peru shelf. In *Modern and Ancient Continental Shelf Anoxia* (eds. R. V. Tyson and T. H. Pearson), pp. 155-170. Geological Society of London.

Emerson S. R. and Huested S. S. (1991) Ocean anoxia and the concentrations of molybdenum and vanadium in seawater. *Mar. Chem.* **34,** 177–196.

Engleman E. E., Jackson L. L., and Norton D. R. (1985) Determination of carbonate carbon in geological materials by coulometric titration. *Chem. Geol*. **53,** 125–128.

Ferdelman T. G., Lee C., Pantoja S., Harder J., Bebout B. M., and Fossing H. (1997) Sulfate reduction and methanogenesis in a *Thioploca*-dominated sediment off the coast of Chile. *Geochim. Cosmochim. Acta* **61** (*15*), 3065–3079.

Fisher N. S. and Wente M. (1993) The release of trace-elements by dying marine phytoplankton. *Deep-Sea Res. I* **40** (*4*), 671–694.

Flegal A. R. and Patterson C. C. (1985) Thallium concentrations in seawater. *Mar. Chem.* **15** (*4*), 327–331.

Flegal A. R., Sanudo-Wilhelmy S. A., and Scelfo G. M. (1995) Silver in the eastern Atlantic Ocean. *Mar. Chem.* **49** (*4*), 315–320.

Fossing H. (1990) Sulfate reduction in shelf sediments in the upwelling region off central Peru. *Continental Shelf Res.* **10** (*4*), 355–367.

Fossing H. and Jørgensen B. B. (1989) Measurement of bacterial sulfate reduction in sediments—Evaluation of a single-step chromium reduction method. *Biogeochemistry* **8** (*3*), 205–222.

Glenn C. R. and Arthur M. A. (1988) Petrology and major element geochemistry of Peru margin phosphorites and associated diagenetic minerals—Authigenesis in modern organic-rich sediments. *Mar. Geol.* **80** (*3–4*), 231–267.

Habicht K. S., Canfield D. E., and Rethmeier J. (1998) Sulfur isotope fractionation during bacterial reduction and disproportionation of thiosulfate and sulfite. *Geochim. Cosmochim. Acta* **62** (*15*), 2585–2595.

Habicht K. S. and Canfield D. E. (2001) Isotope fractionation by sulfate-reducing natural populations and the isotopic composition of sulfide in marine sediments. *Geology* **29** (*6*), 555–558.

Hart T. J. and Currie R. I. (1960) The Benguela current. *Discovery Rep*. **31,** 123–398.

Hartmann M. (1964) Zur Geochemie von Mangan und Eisen in der Ostsee. *Meyniana* **14,** 3.

Hartmann M. and Nielsen H. (1969) $\delta^{34}$S-Werte in rezenten Meeressedimenten und ihre Deutung am Beispiel einiger Sedimentprofile aus der westlichen Ostsee. *Geol. Rundschau* **58,** 621–655.

Heggie D. and Lewis T. (1984) Cobalt in pore waters of marine sediments. *Nature* **311,** 453–455.

Heinrichs H., Schulz-Dobrick B., and Wedepohl K. H. (1980) Terrestrial geochemistry of Cd, Bi, Tl, Pb, Zn, Rb. *Geochim. Cosmochim. Acta* **44,** 1519–1533.

Heinrichs H., Brumsack H. J., Loftfield N., and König N. (1986) Verbessertes Druckaufschlußsystem für biologische und anorganische Materialien. *Z. Pflanzenernährung Bodenkunde* **149,** 350–353.

Heinrichs H. and Hermann A. G. (1990) *Praktikum der Analytischen Geochemie*. Springer Verlag.

Heinze W. and Wefer G. (1992) The history of coastal upwelling off Peru (11°S, ODP Leg 112, Site 680B) over the past 650,000 years. In *Upwelling Systems: Evolution Since the Early Miocene,* Vol. 64 (eds. C. P. Summerhayes, W. L. Prell, and K.-C. Emeis), pp. 451-462. Special Publication. Geological Society.

Helz G. R., Miller C. V., Charnock J. M., Mosselmans J. F. W., Pattrick R. A. D., Garner C. D., and Vaughan D. J. (1996) Mechanism of molybdenum removal from the sea and its concentration in black shales: EFAXS evidence. *Geochim. Cosmochim. Acta* **60** (*19*), 3631–3642.

Hem J. D., Lind C. J., and Robertson C. E. (1989) Coprecipitation and redox reactions of manganese oxide with copper and nickel. *Geochim. Cosmochim. Acta* **53,** 2811–2822.

Hill E. A., Hickey B. M., Shillington F. A., Strub P. T., Brink K. H., Barton E. D. and Thomas A. C. (1998) Eastern ocean boundaries. In *The Global Coastal Ocean—Regional Studies and Syntheses,* Vol. 11 of *The Sea—Ideas and Observations in the Study of the Seas* (eds. A. R. Robinson and K. H. Brink), pp. 29-67. Wiley.

Huerta-Diaz M. A. and Morse J. W. (1992) Pyritization of trace metals in anoxic marine sediments. *Geochim. Cosmochim. Acta* **56,** 2681–2702.

Huffman E. W. D. (1977) Performance of a new automatic carbon dioxide coulometer. *Microchem. J.* **22,** 567–573.

Ingall E. and Jahnke R. (1994) Evidence for enhanced phosphorus regeneration from marine sediments overlain by $O_2$ depleted waters. *Geochim. Cosmochim. Acta* **58,** 2571–2575.

Jørgensen B. B. (1978) Comparison of methods for the quantification of bacterial sulfate reduction in coastal marine-sediments. 1. Measurement with radiotracer techniques. *Geomicrobiol. J.* **1** (*1*), 11–27.

Kaplan I. R. and Rittenberg S. C. (1964) Microbiological fractionation of sulphur isotopes. *J. Gen. Microbiol.* **34** (*2*), 195.

Klinkhammer G. and Palmer M. (1991) Uranium in the oceans: Where it goes and why. *Geochim. Cosmochim. Acta* **55,** 1799–1806.

Knauer G. A., Martin J. H., and Bruland K. W. (1979) Fluxes of particulate carbon, nitrogen, and phosphorus in the upper water column of the northwest Pacific. *Deep-Sea Res.* **26,** 97–108.

Koide M., Hodge V. F., Yang J. S., Stallard M., Goldberg E. G., Calhoun J., and Bertine K. K. (1986) Some comparative marine chemistries of rhenium, gold, silver and molybdenum. *Appl. Geochem.* **1,** 705–714.

Kremling K. (1983) The behavior of Zn, Cd, Cu, Ni, Co, Fe, and Mn in anoxic Baltic waters. *Mar. Chem.* **13** (*2*), 87–108.

Kriete C., Suckow A., and Harazim B. (2004) Meteoric pore water in dated marine sediment cores off Callao, Peru. *Estuar. Coastal Shelf Sci.,* **59** (*3*), 499–510.

Krissek L. A., Scheidegger K. F., and Kulm L. D. (1980) Surface sediments of the Peru-Chile continental-margin and the Nazca Plate. *Geol. Soc. Am. Bull*. **91** (*6*), 321–331.

Kudrass H. R., ed. (2000) *Cruise report SO147 Peru Upwelling: Valparaiso—Callao, 29.05.-03.07.2000.*BGR Hannover, Germany.

Lee D. S., Edmond J. M., and Bruland K. W. (1986) Bismuth in the Atlantic and North Pacific—A natural analog to plutonium and lead. *Earth Planet. Sci. Lett.* **76** (*3–4*), 254–262.

Le Maitre R. W. (1976) Chemical variability of some common igneous rocks. *J. Petrol.* **17** (*4*), 589.

Levin L., Gutierrez D., Rathburn A., Neira C., Sellanes J., Munoz P., Gallardo V., and Salamanca M. (2002) Benthic processes on the Peru margin: A transect across the oxygen minimum zone during the 1997–98 El Nino. *Progr. Oceanogr.* **53** (*1*), 1–27.

Lipinski M., Warning B., and Brumsack H. J. (2003) Trace metal signatures of Jurassic/Cretaceous black shales from the Norwegian Shelf and the Barents Sea. *Palaeogeogr. Palaeoclimatol. Palaeoecol.* **190,** 459–475.

Lückge A., Boussafir M., Lallier-Verges E., and Littke R. (1996) Comparative study of organic matter preservation in immature sediments along the continental margins of Peru and Oman. 1. Results of petrographical and bulk geochemical data. *Org. Geochem.* **24** (*4*), 437–451.

Lückge A. and Reinhardt L. (2000) CTD measurements in the water column off Peru. In *Cruise Report SO147 Peru Upwelling: Valparaiso—Callao, 29.05.-03.07.2000* (ed. H. R. Kudrass) pp. 35-37. BGR Hannover.

Luther G. W. III. (1991) Pyrite synthesis via polysulfide compounds. *Geochim. Cosmochim. Acta* **55,** 2839–2849.

Lyle M. (1981) Formation and growth of ferromanganese oxides on the Nazca Plate. *Geol. Soc. Am. Memoirs* **154,** 269–293.

MacFarlane A. W., Marcet P., Lehuray A. P., and Petersen U. (1990) Lead isotope provinces of the central Andes inferred from ores and crustal rocks. *Econ. Geol. Bull. Soc. Econ. Geol.* **85** (*8*), 1857–1880.

Martin J. H., Knauer G. A., and Gordon R. M. (1983) Silver distributions and fluxes in the north-east Pacific waters. *Nature* **305,** 306–309.

McCaffrey M. A., Farrington J. W., and Repeta D. J. (1990) The organic geochemistry of Peru margin surface sediments 1. A comparison of the c-37 alkenone and historical El Niño records. *Geochim. Cosmochim. Acta* **54** (*6*), 1671–1682.

McKay J. L. and Pedersen T. F. (2000) Geochemical behavior of redox-sensitive trace metals in iron-sulfide layers. *Eos* **81** (*48*), OS52. B-07.

McKay J. L. and Pedersen T. F. (2002) Accumulation of redox-sensitive trace metals in continental margin sediments and their paleo-applications. *Eos* **83,** OS32.B-124.

Molina-Cruz A. (1977) The relation of the southern trade winds to upwelling processes during the last 75,000 years. *Quat. Res*. **8,** 324–339.

Morford J. L. and Emerson S. (1999) The geochemistry of redox sensitive trace metals in sediments. *Geochim. Cosmochim. Acta* **63** (*11–12*), 1735–1750.

Mossmann J. R., Alpin A. C., Curtis C. D., and Coleman M. L. 1991) Geochemistry of inorganic and organic sulfur in organic-rich sediments from the Peru margin. *Geochim. Cosmoch. Acta* **55** (*12*), 3581–3595.

Müller P. J. and Suess E. (1979) Productivity, sedimentation-rate, and sedimentary organic-matter in the oceans 1: Organic-carbon preservation. *Deep-Sea Res. A* **26** (*12*), 1347–1362.

Nameroff T. J., Balistrieri L. S., and Murray J. W. (2002) Suboxic trace metal geochemistry in the eastern tropical North Pacific. *Geochim. Cosmochim. Acta* **66** (*7*), 1139–1158.

Nathan Y., Soudry D., Levy Y., Shitrit D., and Dorfman E. (1997) Geochemistry of cadmium in the Negev phosphorites. *Chem. Geol* **142** (*1–2*), 87–107.

Nijenhuis I. A., Brumsack H.-J., and De Lange G. J. (1998) The trace element budget of the eastern Mediterranean during Pliocene sapropel formation. In *Proceedings of the Ocean Drilling Program, Scientific Results,* Vol. 160 (eds. A. H. F. Robertson, K.-C. Emeis, C. Richter, and A. Camerlenghi), pp. 199-206. Ocean Drilling Program.

Passier H. F., Luther G. W., and De Lange G. J. (1997) Early diagenesis and sulphur speciation in sediments of the Oman Margin, northwestern Arabian Sea. *Deep-Sea Res. II* **44** (*6–7*), 1361–1380.

Passier H. F., Böttcher M. E., and De Lange G. J. (1999) Sulphur enrichment in organic matter of eastern Mediterranean sapropels: A study of sulphur isotope partitioning. *Aquat. Geochem.* **5** (*1*), 99–118.

Pedersen T. F., Shimmield G. B., and Price N. B. (1992) Lack of enhanced preservation of organic-matter in sediments under the oxygen minimum on the Oman Margin. *Geochim. Cosmochim. Acta* **56** (*1*), 545–551.

Prakash Babu C., Brumsack H. J., and Schnetger B. (1999) Distribution of organic carbon in surface sediments along the eastern Arabian Sea: A revisit. *Mar. Geol.* **162** (*1*), 91–103.

Raiswell R. and Canfield D. E. (1996) Rates of reaction between silicate iron and dissolved sulfide in Peru Margin sediments. *Geochim. Cosmochim. Acta* **60** (*15*), 2777–2787.

Reimers C. E. and Suess E. (1983) Spatial and temporal patterns of organic matter accumulation on the Peru continental margin. In *Coastal Upwelling—Its Sediment Record, Part B* (eds. E. Suess and J. Thiede) pp. 311-345. Plenum Press.

Rehkämper M., Frank M., Hein J. R., and Halliday A. (2004) Cenozoic marine geochemistry of thallium deduced from isotopic studies of ferromanganese crusts and pelagic sediments. *Earth Planet. Sci. Lett.* **219** (*1–2*), 77–91.

Reinhardt L., Kudrass H. R., Lückge A., Weidicke M., Wunderlich J., and Wendt G. (2002) High-resolution sediment echosounding off Peru: Late Quaternary depositional sequences and sedimentary structures of a current-dominated shelf. *Marine Geophys. Res.* **23** (*4*), 335–351.

Rosenthal Y., Lam P., Boyle E. A., and Thomson J. (1995) Authigenic cadmium enrichments in suboxic sediments: Precipitation and post-depositional mobility. *Earth Planet. Sci. Lett.* **132,** 99–111.

Sarbas B. (2002) Geochemistry of oceanic island-arc and active continental margin volcanic suites: Some statistical evaluations and implications. Using the database GEOROC. *Eos* **83** (*47*), V62.B-1401.

Schaule B. K. and Patterson C. C. (1981) Lead concentrations in the Northeast Pacific—Evidence for global anthropogenic perturbations. *Earth Planet. Sci. Lett.* **54** (*1*), 97–116.

Schedlbauer O. F. and Heumann K. G. (2000) Biomethylation of thallium by bacteria and first determination of biogenic dimethylthallium in the ocean. *Applied Organometallic Chemistry*. **14** (*6*), 330–340.

Scheidegger K. F. and Krissek L. A. (1982) Dispersal and deposition of eolian and fluvial sediments off Peru and northern Chile. *Geol. Soc. Am. Bull*. **93** (*2*), 150–162.

Scheidegger K. F. and Krissek L. A. (1983) Zooplankton and nekton: Natural barriers to the seaward transport of suspended terrigenous particles off Peru. In *Coastal Upwelling—Its Sediment Record, Part A* (eds. E. Suess and J. Thiede), pp. 303-333. Plenum Press.

Schenau S. J., Passier H. F., Reichart G. J., and de Lange G. J. (2002) Sedimentary pyrite formation in the Arabian Sea. *Mar. Geol.* (3–4), 393–402.

Schnetger B. (1997) Trace element analysis of sediments by HR-ICP-MS using low and medium resolution and different acid digestions. *Fresenius J. Anal. Chem.* **359,** 468–472.

Schnetger B., Brumsack H. J., Schale H., Hinrichs J., and Dittert L. (2000) Geochemical characteristics of deep-sea sediments from the Arabian Sea: A high-resolution study. *Deep-Sea Res. II* **47** (*14*), 2735–2768.

Shaw T. J., Gieskes J. M., and Jahnke R. A. (1990) Early diagenesis in differing environments: The response of transition metals in pore water. *Geochim. Cosmochim. Acta* **54,** 1233–1246.

Shimmield G. B. (1992) Can sediment geochemistry record changes in coastal upwelling paleoproductivity? Evidence from northwest Africa and the Arabian Sea. In *Upwelling Systems: Evolution since the Early Miocene* (eds. C. P. Summerhayes, W. L. Prell and K. C. Emeis), pp. 29-46. Special Publication 64. Geol Soc.

Sillitoe R. H. (2003) Iron oxide-copper-gold deposits: An Andean view. *Mineral. Dep.* **38** (*7*), 787–812.

Suess E. (1981) Phosphate regeneration from sediments of the Peru continental margin by dissolution of fish debris. *Geochim. Cosmochim. Acta* **45** (*4*), 577–588.

Suess E., Kulm L. D. and Killingley J. S. (1986) Coastal upwelling and a history of organic-rich mudstone deposition off Peru. In *Marine Petroleum Source Rocks* (eds. J. Brooks and A. J. Fleet), pp. 181-197. Geological Society.

Suits N. S. and Arthur M. A. (2000) Sulfur diagenesis and partitioning in Holocene Peru shelf and upper slope sediments. *Chem. Geol.* **163** (*1–4*), 219–234.

Thomson J., Higgs N. C., Wilson T. R. S., Croudace I. W., De Lange G. J., and Van Santvoort P. J. M. (1995) Redistribution and geochemical behavior of redox-sensitive elements around S1, the most recent eastern Mediterranean sapropel. *Geochim. Cosmochim. Acta* **59,** 3487–3501.

Veeh H. H. (1967) Deposition of uranium from ocean. *Earth Planet. Sci. Lett.* **3** (*2*), 145.

Vila T., Sillitoe R. H., Betzhold J., and Viteri E. (1991) The porphyry gold deposit at Marte, Northern Chile. *Econ. Geol. Bull. Soc. Econ. Geol.* **86** (*6*), 1271–1286.

Von Breymann M. T., Emeis K. C., and Camerlenghi A. (1990) Geochemistry of sediments from the Peru upwelling area: Results from sites 680, 682, 685, and 688. In *Proceedings of the Ocean Drilling Program, Scientific Results, 112,* Vol. 107 (eds. E. Suess and R. von Huehne), pp. 361-386. Ocean Drilling Program.

Warning B. and Brumsack H. J. (2000) Trace metal signatures of eastern Mediterranean sapropels. *Palaeogeogr. Palaeoclimatol. Palaeoecol.* **158** (*3–4*), 293–309.

Wedepohl K. H. (1971) Environmental influences on the chemical composition of shales and clays. In *Physics and Chemistry of the Earth,* Vol. 8 (eds. L. H. Ahrens, F. Press, S. K. Runcorn and H. C. Urey), pp. 305-333. Pergamon.

Wedepohl K. H. (1991) The composition of the upper earth's crust and the natural cycles of selected metals. Metals in natural raw materials. Natural Resources. In *Metals and Their Compounds in the Environment* (ed. E. Merian), pp. 3-17. VCH.

Wijsman J. W. M., Middelburg J. J., Herman P. M. J., Böttcher M. E., and Heip C. H. R. (2001) Sulfur and iron speciation in surface sediments along the northwestern margin of the Black Sea. *Mar. Chem.* **74** (*4*), 261–278.

Wolf A. (2002) Zeitliche. Variationen im peruanischen Küstenauftrieb seit dem Letzten Glazialen Maximum—Steuerung durch globale Klimadynamik. Ph.D. thesis. Christian-Albrechts-Universität zu Kiel, Germany.

Zheng Y., Anderson R. F., van Geen A., and Kuwabara J. (2000) Authigenic molybdenum formation in marine sediments: A link to pore water sulfide in the Santa Barbara Basin. *Geochim. Cosmochim. Acta* **64** (*24*), 4165–4178.

Zheng Y., Anderson R. F., van Geen A., and Fleisher M. Q. (2002) Preservation of particulate non-lithogenic uranium in marine sediments. *Geochim. Cosmochim. Acta* **66** (*17*), 3085–3092.

Zopfi J., Böttcher M. E., and Jørgensen B. B. (2000) Early diagenesis and isotope biogeochemistry of sulfur in Thioploca-dominated sediments off Chile. In *Sulfide Oxidation and Speciation of Sulfur Intermediates in Marine Environments* (by J. Zopfi), pp. 85–109. Ph.D. thesis. University of Bremen.

Zuta S. and Guillen O. (1970) Oceanografia de las aguas costeras del Peru. *Inst. Mar Peru Bol.* **2,** 162–323.

## APPENDIX

Average contents (0–5 cmbsf) of TIC, TOC, TS, main/trace elements, depth integrated sulfate reduction rates (SRR, 0–20 cmbsf; average of two parallel cores) and element/Al ratios. Water depth (wd) in [m]; AV = average value, SD = standard deviation. TIC, TOC, TS, Si, Ti, Al, Fe, Mg, Ca, K, P in [%], Re in [ppb], other in [ppm], SRR in [mmol · $m^{-2}$ · $d^{-1}$], E/Al ratios are ($\times 10^{-4}$) except Re/Al ($\times 10^{-7}$), Mn/Al, Re/Mo ($\times 10^{-3}$). Data in italics semiquantitative.

| Site/wd | | SRR | TIC | TOC | TS | Si | Ti | Al | Fe | Mg | Ca | K | P | Ag | As |
|---|---|---|---|---|---|---|---|---|---|---|---|---|---|---|---|
| 126MC | AV | 11.9 | 0.35 | 2.03 | 1.01 | 24.5 | 0.43 | 8.73 | 4.63 | 1.71 | 1.62 | 2.16 | 0.11 | 0.51 | 25.8 |
| 85 | SD | | 0.05 | 0.20 | 0.02 | 0.2 | 0.01 | 0.07 | 0.07 | 0.01 | 0.07 | 0.02 | 0.00 | 0.03 | 1.7 |
| 2MC | AV | 10.1 | 0.08 | 6.36 | 1.36 | 23.9 | 0.33 | 6.27 | 3.19 | 1.11 | 1.05 | 1.59 | 0.17 | | 30.3 |
| 86 | SD | | 0.08 | 1.03 | 0.18 | 0.9 | 0.03 | 0.55 | 0.20 | 0.10 | 0.16 | 0.12 | 0.02 | | 2.4 |
| 5MC | AV | 3.9 | 0.10 | 7.03 | 1.26 | 27.1 | 0.29 | 5.78 | 3.34 | 1.08 | 0.93 | 1.36 | 0.17 | 0.75 | 42.3 |
| 96 | SD | | 0.38 | 0.15 | 0.5 | 0.01 | 0.27 | 0.14 | 0.06 | 0.20 | 0.03 | 0.02 | 0.06 | 12.1 | |
| 29MC | AV | | 0.13 | 7.89 | 1.30 | 24.7 | 0.32 | 6.36 | 2.92 | 0.92 | 0.95 | 1.43 | 0.20 | 0.40 | 29.1 |
| 102 | SD | | 0.18 | 1.67 | 0.12 | 0.5 | 0.09 | 1.58 | 0.47 | 0.21 | 0.12 | 0.27 | 0.03 | 0.05 | 2.2 |
| 120MC | AV | 1.3 | 1.3 | 9.78 | 1.52 | 24.6 | 0.29 | 6.08 | 3.07 | 1.18 | 1.29 | 1.46 | 0.21 | | 27.7 |
| 115 | SD | | 0.25 | 1.81 | 0.26 | 0.8 | 0.04 | 0.81 | 0.34 | 0.16 | 0.35 | 0.15 | 0.04 | | 2.5 |
| 45MC | AV | 3.1 | 0.38 | 20.7 | 2.05 | 15.9 | 0.19 | 3.89 | 1.57 | 0.79 | 1.17 | 0.94 | 0.33 | 0.97 | 29.6 |
| 153 | SD | | 0.40 | 0.50 | 0.13 | 1.0 | 0.03 | 0.66 | 0.21 | 0.09 | 0.48 | 0.10 | 0.02 | 0.05 | 3.0 |
| 104MC | AV | 3.1 | 0.90 | 16.8 | 1.74 | 17.9 | 0.21 | 3.98 | 1.92 | 0.87 | 2.76 | 1.33 | 0.31 | | 30.9 |
| 185 | SD | | 0.33 | 1.0 | 0.28 | 0.6 | 0.02 | 0.43 | 0.05 | 0.08 | 0.61 | 0.10 | 0.05 | | 2.6 |
| 71MC | AV | 0.2 | 3.48 | 19.5 | 0.74 | 7.4 | 0.11 | 2.36 | 0.93 | 0.61 | 7.03 | 0.58 | 0.37 | 0.86 | 15.2 |
| 239 | SD | | 0.28 | 1.2 | 0.06 | 0.5 | 0.01 | 0.15 | 0.05 | 0.02 | 0.51 | 0.04 | 0.06 | 0.31 | 1.1 |
| 18MC | AV | 1.9 | 0.30 | 20.6 | 1.34 | 17.7 | 0.22 | 4.35 | 1.84 | 0.83 | 1.27 | 1.07 | 0.31 | | 29.0 |
| 255 | SD | | 0.20 | 1.3 | 0.15 | 0.4 | 0.03 | 0.36 | 0.25 | 0.05 | 0.41 | 0.16 | 0.05 | | 2.6 |
| 8MC | AV | | 1.15 | 14.4 | 0.92 | 21.6 | 0.26 | 5.06 | 1.96 | 0.86 | 1.68 | 1.22 | 0.45 | 0.75 | 22.1 |
| 282 | SD | | 0.81 | 1.4 | 0.19 | 3.3 | 0.09 | 1.23 | 0.48 | 0.15 | 0.61 | 0.28 | 0.43 | 0.07 | 2.8 |
| 1MC | AV | 0.3 | 0.97 | 21.3 | 1.53 | 15.5 | 0.18 | 3.41 | 1.49 | 0.66 | 2.14 | 0.70 | 0.29 | | 22.4 |
| 321 | SD | | 0.85 | 4.3 | 0.16 | 2.2 | 0.04 | 0.83 | 0.28 | 0.12 | 1.33 | 0.12 | 0.03 | | 3.2 |
| 122MC | AV | 0.1 | 1.00 | 20.6 | 1.02 | 13.7 | 0.17 | 3.53 | 1.40 | 0.86 | 2.58 | 0.91 | 0.39 | | 19.1 |
| 364 | SD | | 1.22 | 3.1 | 0.20 | 0.8 | 0.03 | 0.63 | 0.20 | 0.06 | 1.58 | 0.11 | 0.03 | | 1.3 |
| 35MC | AV | 0.4 | 4.04 | 6.2 | 0.80 | 16.7 | 0.18 | 3.79 | 2.00 | 0.92 | 9.50 | 1.11 | 1.95 | 0.92 | 11.6 |
| 598 | SD | | 1.64 | 0.9 | 0.12 | 5.4 | 0.06 | 1.08 | 0.24 | 0.16 | 3.67 | 0.27 | 0.53 | 0.14 | 3.0 |
| 14MC | AV | 0.3 | 7.73 | 5.6 | 0.14 | 7.0 | 0.09 | 1.86 | 1.23 | 0.47 | 15.3 | 0.62 | 0.38 | 0.23 | *<10* |
| 654 | SD | | 0.47 | 0.9 | 0.03 | 0.6 | 0.01 | 0.14 | 0.07 | 0.04 | 0.79 | 0.02 | 0.13 | 0.03 | |
| 81MC | AV | 0.3 | 1.78 | 3.1 | 0.26 | 20.3 | 0.16 | 3.56 | 8.82 | 1.64 | 4.83 | 3.23 | 1.03 | 0.41 | 14.2 |

**APPENDIX.** (Continued)

| Site/wd | | SRR | TIC | TOC | TS | Si | Ti | Al | Fe | Mg | Ca | K | P | Ag | As |
|---|---|---|---|---|---|---|---|---|---|---|---|---|---|---|---|
| 1278 | SD | | 0.11 | 0.5 | 0.05 | 0.4 | 0.01 | 0.16 | 0.79 | 0.08 | 0.27 | 0.25 | 0.10 | 0.09 | 0.7 |
| 33MC | AV | 0.5 | 1.61 | 6.4 | 0.27 | 21.9 | 0.31 | 5.49 | 3.66 | 1.10 | 3.82 | 1.63 | 0.30 | 1.23 | *<10* |
| 1357 | SD | | 0.03 | 0.1 | 0.11 | 0.2 | 0.00 | 0.07 | 0.10 | 0.04 | 0.08 | 0.05 | 0.00 | 0.03 | |

| Site/wd | | Bi | Cd | Co | Cr | Cu | Mn | Mo | Ni | Pb | Rb | Re | Sb | Tl | U | V | Zn | Zr |
|---|---|---|---|---|---|---|---|---|---|---|---|---|---|---|---|---|---|---|
| 126MC | AV | 0.58 | 5.0 | 15.0 | 28 | 98.4 | 697 | 22 | 17 | 57.2 | 117 | 11.3 | 3.1 | 1.40 | 4.4 | 156 | 193 | 130 |
| 85 | SD | 0.02 | 1.0 | 0.2 | 1 | 3.8 | 10 | 6 | 2 | 1.6 | 2 | 11.2 | 0.2 | 0.12 | 0.6 | 12 | 2 | 3 |
| 2MC | AV | | | | 90 | 54.5 | 306 | 40 | 41 | 37.1 | 84 | | | | 6.6 | 174 | 144 | 115 |
| 86 | SD | | | | 12 | 1.6 | 37 | 12 | 6 | 3.5 | 9 | | | | 3.0 | 43 | 10 | 11 |
| 5MC | AV | 0.70 | 42.8 | 7.6 | 99 | 82.8 | 339 | 66 | 46 | 72.4 | 79 | 13.9 | 3.0 | 2.65 | 6.5 | 184 | 231 | 84 |
| 96 | SD | 0.08 | 5.0 | 0.6 | 11 | 1.9 | 17 | 4 | 2 | 2.3 | 5 | 3.5 | 0.3 | 0.51 | 0.9 | 35 | 8 | 4 |
| 29MC | AV | 0.49 | 37.7 | 7.0 | 99 | 56.6 | 283 | 51 | 47 | 32.2 | 76 | 20.6 | 2.7 | 2.21 | 7.3 | 155 | 137 | 118 |
| 102 | SD | 0.09 | 3.5 | 1.5 | 10 | 7.7 | 93 | 12 | 2 | 4.3 | 20 | 8.4 | 0.4 | 0.76 | 3.0 | 39 | 27 | 38 |
| 120MC | AV | | | | 105 | 73.4 | 371 | 74 | 64 | 37.0 | 79 | | | | 17.8 | 250 | 149 | 85 |
| 115 | SD | | | | 22 | 4.5 | 51 | 24 | 16 | 7.1 | 11 | | | | 2.7 | 37 | 7 | 13 |
| 45MC | AV | 0.31 | 80.5 | 5.0 | 138 | 59.0 | 157 | 96 | 118 | 21.3 | 44 | 106 | 3.1 | 1.71 | 18.5 | 166 | 109 | 76 |
| 153 | SD | 0.05 | 3.7 | 0.3 | 17 | 10.4 | 25 | 10 | 18 | 0.7 | 6 | 6.4 | 0.2 | 0.33 | 2.1 | 63 | 10 | 15 |
| 104MC | AV | 0.35 | 59.7 | 5.2 | 148 | 83.6 | 159 | 96 | 127 | 27.0 | 45 | 68.5 | 4.8 | 1.56 | 13.4 | 281 | 130 | 71 |
| 185 | SD | 0.04 | 1.5 | 0.8 | 13 | 10.5 | 19 | 20 | 18 | 2.7 | 4 | 10.6 | 0.1 | 0.14 | 1.5 | 91 | 7 | 5 |
| 71MC | AV | 0.21 | 22.3 | 3.9 | 119 | 53.7 | 95 | 40 | 130 | 10.8 | 31 | 121 | 3.7 | 0.48 | 20.8 | 178 | 97 | 44 |
| 239 | SD | 0.08 | 2.8 | 0.2 | 10 | 6.1 | 8 | 13 | 10 | 3.5 | 2 | 15.2 | 1.2 | 0.13 | 5.5 | 53 | 2 | 4 |
| 18MC | AV | | | | 140 | 89.9 | 146 | 117 | 152 | 28.9 | 56 | | | | 26.2 | 419 | 148 | 73 |
| 255 | SD | | | | 22 | 13.0 | 25 | 29 | 32 | 4.6 | 26 | | | | 6.5 | 79 | 14 | 15 |
| 8MC | AV | 0.23 | 45.7 | 3.4 | 122 | 53.0 | 244 | 53 | 101 | 18.7 | 58 | 46.2 | 3.7 | 1.38 | 17.8 | 210 | 115 | 112 |
| 282 | SD | 0.05 | 12.4 | 0.8 | 13 | 10.3 | 75 | 18 | 18 | 3.3 | 14 | 11.2 | 0.4 | 0.53 | 4.9 | 70 | 6 | 45 |
| 1MC | AV | | | | 144 | 82.7 | 112 | 39 | 179 | 15.3 | 34 | | | | 31.4 | 458 | 132 | 55 |
| 321 | SD | | | | 23 | 18.2 | 44 | 8 | 45 | 2.3 | 6 | | | | 13.9 | 176 | 16 | 10 |
| 122MC | AV | | | | 151 | 59.3 | 177 | 57 | 158 | 13.3 | 44 | | | | 34.3 | 377 | 122 | 69 |
| 364 | SD | | | | 27 | 11.2 | 27 | 9 | 32 | 2.1 | 6 | | | | 9.8 | 95 | 15 | 11 |
| 35MC | AV | 0.20 | 9.1 | 3.9 | 122 | 40.6 | 167 | 27 | 54 | 16.2 | 52 | 60.6 | 1.9 | 1.37 | 31.0 | 87 | 97 | 90 |
| 598 | SD | 0.07 | 2.5 | 1.2 | 9 | 7.6 | 57 | 5 | 5 | 3.2 | 14 | 20.2 | 0.3 | 0.35 | 3.2 | 24 | 7 | 21 |
| 14MC | AV | 0.08 | 2.0 | 2.3 | 92 | 42.6 | 24 | 2.2 | 49 | 5.0 | 23 | 40.1 | 1.1 | 0.22 | 6.7 | 37 | 73 | 56 |
| 654 | SD | 0.01 | 0.2 | 0.1 | 1 | 3.3 | 7 | 0.4 | 6 | 0.7 | 2 | 3.7 | 0.1 | 0.02 | 1.3 | 2 | 7 | 5 |
| 81MC | AV | 0.09 | 1.6 | 3.0 | 297 | 39.4 | 129 | 1.2 | 41 | 6.3 | 119 | 17.1 | 2.3 | 0.61 | 16.3 | 127 | 95 | 109 |
| 1278 | SD | 0.02 | 0.1 | 0.3 | 22 | 6.7 | 16 | 0.1 | 4 | 0.7 | 6 | 2.4 | 0.2 | 0.02 | 2.3 | 6 | 6 | 7 |
| 33MC | AV | 0.19 | 0.9 | 5.4 | 128 | 52.2 | 191 | 1.2 | 77 | 10.2 | 80 | 22.7 | 1.5 | 0.51 | 5.8 | 88 | 136 | 151 |
| 1357 | SD | 0.06 | 0.1 | 0.1 | 4 | 1.6 | 2 | 0.1 | 4 | 0.5 | 1 | 1.3 | 0.1 | 0.01 | 0.2 | 2 | 3 | 3 |

| Site/wd | | Ag/Al | As/Al | Bi/Al | Cd/Al | Co/Al | Cr/Al | Cu/Al | Mn/Al | Mo/Al |
|---|---|---|---|---|---|---|---|---|---|---|
| 126MC | AV | 0.059 | 2.96 | 0.067 | 0.58 | 1.72 | 3.2 | 11.3 | 10.3 | 2.55 |
| 85 | SD | 0.004 | 0.20 | 0.003 | 0.11 | 0.03 | 0.1 | 0.5 | 0.2 | 0.73 |
| 2MC | AV | | 4.88 | | | | 14.5 | 8.7 | 6.3 | 6.47 |
| 86 | SD | | 0.78 | | | | 2.0 | 0.8 | 0.2 | 2.51 |
| 5MC | AV | 0.130 | 7.40 | 0.121 | 7.38 | 1.31 | 17.1 | 14.3 | 7.6 | 11.41 |
| 96 | SD | 0.006 | 2.50 | 0.008 | 0.54 | 0.04 | 1.2 | 0.5 | 0.1 | 0.52 |
| 29MC | AV | 0.068 | 5.04 | 0.082 | 6.58 | 1.15 | 16.2 | 9.2 | 5.6 | 9.17 |
| 102 | SD | 0.017 | 2.34 | 0.015 | 2.53 | 0.17 | 3.7 | 1.8 | 0.7 | 5.92 |
| 120MC | AV | | 4.64 | | | | 17.4 | 12.2 | 7.9 | 12.20 |
| 115 | SD | | 0.98 | | | | 3.1 | 1.4 | 0.3 | 3.62 |
| 45MC | AV | 0.235 | 7.76 | 0.076 | 19.56 | 1.20 | 35.8 | 15.3 | 5.2 | 25.89 |
| 153 | SD | 0.011 | 1.02 | 0.012 | 0.78 | 0.07 | 3.1 | 1.7 | 0.2 | 9.18 |
| 104MC | AV | | 7.90 | 0.084 | 14.37 | 1.24 | 37.5 | 21.3 | 5.2 | 24.61 |
| 185 | SD | | 1.36 | 0.000 | 1.99 | 0.04 | 5.0 | 4.1 | 0.2 | 6.47 |
| 71MC | AV | 0.364 | 6.47 | 0.087 | 9.27 | 1.62 | 50.4 | 22.9 | 5.2 | 17.14 |
| 239 | SD | 0.149 | 0.81 | 0.035 | 1.61 | 0.10 | 4.5 | 3.2 | 0.2 | 5.27 |
| 18MC | AV | | 6.72 | | | | 32.3 | 20.8 | 4.3 | 27.30 |
| 255 | SD | | 0.91 | | | | 5.0 | 3.2 | 0.5 | 7.89 |
| 8MC | AV | 0.177 | 4.66 | 0.053 | 10.90 | 0.79 | 25.3 | 11.2 | 6.1 | 11.54 |
| 282 | SD | 0.075 | 1.38 | 0.023 | 6.13 | 0.34 | 5.4 | 3.8 | 0.5 | 5.56 |
| 1MC | AV | | 6.75 | | | | 43.0 | 24.5 | 4.1 | 11.45 |
| 321 | SD | | 0.95 | | | | 4.5 | 1.7 | 0.8 | 1.04 |
| 122MC | AV | | 5.54 | | | | 42.9 | 16.8 | 6.5 | 16.25 |
| 364 | SD | | 0.81 | | | | 1.5 | 1.3 | 0.2 | 1.01 |
| 35MC | AV | 0.264 | 3.13 | 0.055 | 2.56 | 1.10 | 35.3 | 11.5 | 5.6 | 7.33 |
| 598 | SD | 0.038 | 0.63 | 0.006 | 0.16 | 0.06 | 12.7 | 4.0 | 0.4 | 1.40 |

**APPENDIX.** (Continued)

| Site/wd | | Ag/Al | As/Al | Bi/Al | Cd/Al | Co/Al | Cr/Al | Cu/Al | Mn/Al | Mo/Al |
|---|---|---|---|---|---|---|---|---|---|---|
| 14MC | AV | 0.126 | <2 | 0.040 | 1.06 | 1.25 | 49.5 | 22.9 | 1.7 | 1.18 |
| 654 | SD | 0.016 | | 0.005 | 0.13 | 0.03 | 3.5 | 1.4 | 0.3 | 0.11 |
| 81MC | AV | 0.114 | 4.01 | 0.026 | 0.45 | 0.83 | 83.8 | 11.0 | 4.6 | 0.34 |
| 1278 | SD | 0.019 | 0.37 | 0.003 | 0.06 | 0.06 | 9.7 | 1.4 | 0.4 | 0.03 |
| 33MC | AV | 0.224 | <2 | 0.034 | 0.16 | 0.99 | 23.3 | 9.5 | 4.5 | 0.22 |
| 1357 | SD | 0.007 | | 0.011 | 0.03 | 0.01 | 1.0 | 0.4 | 0.0 | 0.01 |

| Site/wd | | Ni/Al | Pb/Al | Re/Al | Sb/Al | Tl/Al | U/Al | V/Al | Zn/Al | Zr/Al | Re/Mo |
|---|---|---|---|---|---|---|---|---|---|---|---|
| 126MC | AV | 1.91 | 6.56 | 1.29 | 0.35 | 0.16 | 0.51 | 17.9 | 22.1 | 14.9 | 1.03 |
| 85 | SD | 0.20 | 0.20 | 1.26 | 0.03 | 0.02 | 0.07 | 1.5 | 0.3 | 0.4 | 1.08 |
| 2MC | AV | 6.66 | 5.97 | | | | 1.08 | 28.2 | 23.1 | 18.3 | |
| 86 | SD | 1.24 | 1.06 | | | | 0.54 | 8.8 | 3.4 | 0.9 | |
| 5MC | AV | 7.92 | 12.55 | 2.39 | 0.52 | 0.46 | 1.13 | 32.1 | 40.1 | 14.5 | 0.22 |
| 96 | SD | 0.45 | 0.73 | 0.49 | 0.02 | 0.12 | 0.23 | 7.7 | 2.4 | 0.2 | 0.03 |
| 29MC | AV | 7.92 | 5.26 | 3.22 | 0.48 | 0.42 | 1.45 | 27.9 | 22.0 | 18.1 | 0.44 |
| 102 | SD | 2.45 | 1.02 | 0.62 | 0.26 | 0.32 | 1.25 | 18.1 | 2.4 | 2.4 | 0.22 |
| 120MC | AV | 10.54 | 6.22 | | | | 2.99 | 42.2 | 24.8 | 14.0 | |
| 115 | SD | 2.14 | 1.65 | | | | 0.74 | 12.0 | 3.7 | 0.5 | |
| 45MC | AV | 30.43 | 5.18 | 25.87 | 0.76 | 0.41 | 5.01 | 48.9 | 28.5 | 19.6 | 0.88 |
| 153 | SD | 1.84 | 0.17 | 1.46 | 0.04 | 0.08 | 1.76 | 41.5 | 3.8 | 1.8 | 0.05 |
| 104MC | AV | 32.33 | 6.45 | 16.31 | 1.16 | 0.38 | 3.19 | 72.2 | 32.9 | 18.1 | 0.77 |
| 185 | SD | 5.85 | 0.09 | 0.69 | 0.11 | 0.08 | 0.00 | 26.9 | 3.6 | 1.1 | 0.11 |
| 71MC | AV | 55.35 | 4.48 | 50.36 | 1.54 | 0.20 | 8.84 | 76.7 | 41.3 | 18.7 | 2.85 |
| 239 | SD | 6.15 | 1.56 | 7.61 | 0.57 | 0.06 | 2.36 | 27.6 | 2.8 | 0.8 | 0.69 |
| 18MC | AV | 35.28 | 6.66 | | | | 6.10 | 97.6 | 34.2 | 16.8 | |
| 255 | SD | 7.69 | 1.04 | | | | 1.63 | 22.4 | 3.3 | 2.9 | |
| 8MC | AV | 21.57 | 4.37 | 10.54 | 0.88 | 0.32 | 3.79 | 46.8 | 24.0 | 21.4 | 0.95 |
| 282 | SD | 8.39 | 1.92 | 3.57 | 0.35 | 0.17 | 1.56 | 28.2 | 5.8 | 3.8 | 0.33 |
| 1MC | AV | 52.59 | 4.69 | | | | 8.85 | 130.6 | 39.7 | 16.3 | |
| 321 | SD | 4.03 | 1.20 | | | | 1.99 | 22.3 | 5.4 | 1.5 | |
| 122MC | AV | 44.81 | 3.82 | | | | 9.58 | 105.8 | 34.8 | 19.7 | |
| 364 | SD | 2.34 | 0.69 | | | | 1.26 | 10.5 | 3.4 | 0.5 | |
| 35MC | AV | 15.09 | 4.61 | 16.77 | 0.53 | 0.39 | 8.94 | 22.9 | 27.1 | 24.1 | 2.31 |
| 598 | SD | 3.57 | 0.35 | 1.70 | 0.05 | 0.03 | 3.24 | 1.3 | 6.4 | 1.6 | 0.71 |
| 14MC | AV | 26.44 | 2.66 | 21.69 | 0.60 | 0.12 | 3.64 | 20.0 | 39.4 | 30.0 | 18.55 |
| 654 | SD | 1.79 | 0.19 | 3.13 | 0.05 | 0.02 | 0.77 | 1.5 | 2.2 | 2.1 | 3.77 |
| 81MC | AV | 11.37 | 1.77 | 4.81 | 0.64 | 0.17 | 4.61 | 35.8 | 26.6 | 30.5 | 14.11 |
| 1278 | SD | 0.77 | 0.14 | 0.71 | 0.07 | 0.01 | 0.75 | 3.3 | 0.5 | 0.9 | 1.22 |
| 33MC | AV | 14.02 | 1.86 | 4.14 | 0.27 | 0.09 | 1.05 | 16.0 | 24.8 | 27.4 | 19.10 |
| 1357 | SD | 0.46 | 0.09 | 0.27 | 0.02 | 0.002 | 0.04 | 0.4 | 0.7 | 0.6 | 2.06 |